VLASOV-POISSON-FOKKER-PLANCK EQUATION IN THE ADIABATIC ASYMPTOTICS

ETIENNE LEHMAN AND CLAUDIA NEGULESCU

ABSTRACT. The main concern of this article is the study of a nonlinear Vlasov-Poisson-Fokker-Planck equation describing the electron dynamics in a thermonuclear fusion plasma, in the regime of a small electron-to-ion mass ratio ($\varepsilon \ll 1$). The first part of this work focuses on the rigorous $\varepsilon \to 0$ asymptotic study, based on hypocoercive techniques, permitting to understand the transition from the kinetic level to the macroscopic, adiabatic electron level. The second part introduces a Hilbert-Fourier spectral method enabling to treat without too much numerical effort the above mentioned electron transition. This scheme has in particular the nice property of being *Asymptotic Preserving* in the sense that ε-independent meshes can be chosen, without degrading the accuracy. Some numerical tests are finally performed validating on one hand the scheme and underscoring on the other hand the mathematical results.

Keywords: Plasma modelling, Vlasov-Poisson-Fokker-Planck equation, adiabatic electron regime, asymptotic analysis, entropy-methods, multi-scale numerical scheme, Asymptotic-Preserving schemes.

1. INTRODUCTION/MOTIVATION

The concern of the present work is the study of the $\varepsilon \to 0$ asymptotic limit of the following coupled, nonlinear $1D_x\,1D_v$ Vlasov-Poisson-Fokker-Planck model

$$(V)_\varepsilon \quad \begin{cases} \partial_t f^\varepsilon + \dfrac{1}{\varepsilon}\, v\, \partial_x f^\varepsilon - \dfrac{1}{\varepsilon}\, E^\varepsilon\, \partial_v f^\varepsilon = \dfrac{1}{\varepsilon}\partial_v \left[v\, f^\varepsilon + \partial_v f^\varepsilon \right] , \\ -\partial_{xx}\phi^\varepsilon = n_i - n^\varepsilon, \qquad E^\varepsilon = -\partial_x \phi^\varepsilon , \end{cases} \tag{1}$$

associated with an initial condition $f^\varepsilon(t=0,\cdot,\cdot) = f^\varepsilon_{in}$ and evolving on the phase-space $(x,v) \in \mathbb{T}_x \times \mathbb{R}_v$ with $\mathbb{T}_x$ a periodic domain. System (1) describes the time evolution of the electron distribution function $f^\varepsilon(t,x,v)$ in a thermonuclear fusion plasma, where the ions are assumed to form a fixed background interacting with the electrons only via the self-consistent electric field E^ε. The given ion density $n_i(t,x)$ is considered time-dependent and sufficiently smooth, *typically* $n_i \in W^{1,\infty}((0,T);L^1(\mathbb{T}_x))$. The small parameter $\varepsilon \in (0,1)$ is related to the small electron-to-ion mass ratio and the asymptotic regime $\varepsilon \ll 1$ corresponds to a situation where the electron dynamics is very fast as compared to the ion motion, which fixes the reference time-scale in current simulations [9, 10, 16, 24]. In particular, to avoid the cumbersome resolution of an electron kinetic equation, present codes describe the electron dynamics through the so-called *electron Boltzmann relation*

$$n(t,x) = c(t)\, e^{\phi(t,x)}\,, \qquad \forall (t,x) \in \mathbb{R}_+ \times \mathbb{T}_x\,, \tag{2}$$

with $c(t)$ defined by the mass constraint $\int_{\mathbb{T}_x} n(t,x)\,\mathrm{d}x = \int_{\mathbb{T}_x} n_i(t,x)\,\mathrm{d}x = \mathfrak{m}$. This relation (2) says that in the regime of a small mass ratio $\varepsilon \ll 1$, the electrons tend towards a thermodynamic equilibrium relating directly the electron equilibrium density to the electric potential. The validity of this adiabatic electron model is however rather controversial. Indeed, this model seems to break down in some situations, as for example near the edge of the tokamak [13]. Unusual electron temperature enhancement are observed when using this relation to describe the electron dynamics rather than a fully kinetic model. It is hence of first importance to understand the asymptotic

Date: September 12, 2022.

passage from the kinetic (mesoscopic) model (1) towards the adiabatic (macroscopic) one (2) and to propose some corrections. For more details about the scaling of the electron kinetic model (1) we refer the interested reader to [14, 26].

The asymptotic limit $\varepsilon \to 0$ of (1) is a singular limit, thus the theoretical as well as numerical investigations are rather complex. Different scalings are usually studied in literature, for example the hydrodynamic scaling, studied for instance in [30], which is based on the equation

$$\partial_t f^\varepsilon + v\,\partial_x f^\varepsilon - E^\varepsilon\,\partial_v f^\varepsilon = \frac{1}{\varepsilon}\mathcal{C}(f^\varepsilon)\,,$$

where $\mathcal{C}$ is some collision operator. One encounters often also the drift-diffusive regime [1, 17, 29], based on the following scaling

$$\partial_t f^\varepsilon + \frac{1}{\varepsilon}\,v\,\partial_x f^\varepsilon - \frac{1}{\varepsilon}\,E^\varepsilon\,\partial_v f^\varepsilon = \frac{1}{\varepsilon^2}\mathcal{C}(f^\varepsilon)\,.$$

Our present scaling (1) is a different one, the main particularity coming from the fact that the collision (diffusive) operator acts at the same order as the transport (mixing) operator, leading to a more delicate struggle between these two very different operators.

In this paper, we shall firstly focus on a rigorous obtention of the electron Boltzmann relation (2) starting from the fully kinetic model (1) and performing the adiabatic asymptotic limit $\varepsilon \to 0$. Our rigorous treatment uses the tools of *hypocoercivity theory*. More precisely, we decide to follow the so-called *"Auxiliary operator method"* [1, 12, 20, 21] build upon a weighted L^2-setting. Usually, hypocoercivity is a tool useful in the study of the long time asymptotics $t \to \infty$, but we adapt it to our needs, especially for time-dependent ion-densities n_i, in which case the limit $\varepsilon \to 0$ of (1) is not equivalent to the long time asymptotics. We underline that other approaches also exist, set down for instance in a H^1-framework [33], in a H^{-1}-setting [2, 7] or in a general H^s-setting [22]. For some introductory material on hypocoercivity theory, one may read [20, 33].

The present analysis is carried out in a Hermite spectral formalism. Specifically, let us denote by $\mathcal{M}(v) := \frac{1}{\sqrt{2\pi}} e^{-v^2/2}$ a Gaussian velocity distribution function and introduce the following weighted measures $\mathrm{d}\gamma(v) := \mathcal{M}^{-1}(v)\,\mathrm{d}v$ on $\mathbb{R}_v$ as well as $\mathrm{d}\sigma(x,v) := \mathrm{d}x\,\mathrm{d}\gamma(v)$ on $\mathbb{T}_x \times \mathbb{R}_v$. Furthermore we shall denote for a measured space $(\Omega, \mathrm{d}\mu)$, by $L^2_\mu(\Omega)$ and $H^s_\mu(\Omega)$ respectively the L^2- and H^s-spaces associated with the measure $\mathrm{d}\mu$. With this, we expand our particle distribution function f^ε, solution of (1), in a Hermite basis corresponding to the velocity variable v

$$f^\varepsilon(t,x,v) = \sum_{k\geqslant 0} C_k^\varepsilon(t,x)\psi_k(v), \tag{3}$$

where $\{\psi_k\}_{k\in\mathbb{N}}$ are well-chosen Hermite functions, forming a complete, orthonormal basis of $L^2_\gamma(\mathbb{R}_v)$ and defined in Section 4.1. There are several advantages, when using a Hermite spectral method for the discretization of the velocity variable. Firstly the functions $\{\psi_k\}_{k\in\mathbb{N}}$ form a complete, orthonormal basis of $L^2_\gamma(\mathbb{R}_v)$ with respect to the Gaussian weights, such that these basis functions seem to be optimal to approach Maxwellian-like distribution functions in v. Secondly, the lower-order terms in the expansion (3) are related to the low-order moments of the distribution function f^ε, namely to the macroscopic quantites like density, momentum and energy, quantities which are usually of interest. Thus, such a Hermite spectral method will permit somehow to make the link between the kinetic and the fluid descriptions, and is particularly well suited for our asymptotic study $\varepsilon \to 0$.

The idea to describe the particle density function as an (infinite) sum of orthogonal polynomials related to the Maxwellian form of the equilibrium is not new. In [8], the author used Sonine's polynomials, in order to simplify the integral forms of collision operators, and in [18], the author used N-dimensional Hermite polynomials to approximate the particle density function, solution of the Boltzmann equation. The use of such type of Hermite expansions for the numerical resolution of

$1D_x\,1D_v$ Vlasov-Poisson equations goes back as soon as the end of the 60's [3,19]. The community then lost interest in these methods, as the computational capacities of that time were not enough to compute - with a high resolution - systems like Vlasov-Poisson. However, in the last decades, these techniques regained interest, and were widely studied and used in the design of numerical schemes [4,15,28,31,32].

Our idea to use a Hermite-decomposition in the velocity variable is related to our aim to study theoretically as well as numerically the adiabatic electron asymptotics $\varepsilon \to 0$ of the kinetic model (1). We performed a mathematical analysis of the asymptotic behaviour of f^ε and deduced some rates of convergence of each Hermite coefficient of the decomposition : the higher the coefficient in the Hermite hierarchy, the faster the convergence, in more details we shall show that $C_k^\varepsilon = \mathcal{O}(\sqrt{\frac{\varepsilon}{k}})$ in some specific norm. This idea is illustrated in [14] and justifies that the Hermite spectral method is particularly well adapted for this kinetic-to-adiabatic transition, as one may neglect for small ε the high order coefficients in the hierarchy, fact which will lead to large computational savings.

In a second time, we design a Hermite-Fourier-Implicit-Euler numerical scheme for (1) and investigate its main features in the regime of a reasonably small $\varepsilon \ll 1$. In particular, we measure accurately the decay rate of several Hermite coefficients with respect to ε as well as to their height in the hierarchy. This numerical scheme will however, at first, not be designed to efficiently handle the singular limit $\varepsilon \to 0$, due to the still present time-stiffness.

We finally dedicate the last part of this article to the modification of the above-mentioned scheme, to construct an efficient *Asymptotic Preserving* (AP) method to manage finally this asymptotic $\varepsilon \to 0$ passage on the discrete level, and this without extensive numerical efforts. An AP scheme has the essential property of being uniformly stable and accurate with respect to a small parameter -in our case ε- and this for a fixed grid. For a complete introduction to the subject, the interested reader may read [23,25].

1.1. Main results.

Let us summarize here the main results of the mathematical analysis of this paper. Firstly a formal asymptotic analysis is carried out to identify the $\varepsilon \to 0$ adiabatic regime of (1). In this limit $\varepsilon \to 0$, the electron particle distribution function converges towards a Maxwellian distribution of the form $n^0(t,x)\mathcal{M}(v)$.

Theorem 1. ***(Limit model)*** *Let $(f^\varepsilon, E^\varepsilon)$ be a solution to (1), for each fixed $\varepsilon > 0$, satisfying the mass constraint*

$$\int_{\mathbb{R}_v}\int_{\mathbb{T}_x} f^\varepsilon(t,x,v)\,\mathrm{d}v\,\mathrm{d}x = \mathfrak{m}\,, \qquad \forall (x,v) \in \mathbb{T}_x \times \mathbb{R}_v\,.$$

Then, the $\varepsilon \to 0$ asymptotic limit (f^0, E^0) is given by the following nonlinear, elliptic ***Limit-model***

$$(L)\quad \begin{cases} f^0(t,x,v) = c(t)\; e^{\phi^0(t,x)}\,\mathcal{M}(v)\,, & c(t) = \mathfrak{m}/\displaystyle\int_{\mathbb{T}_x} e^{\phi^0(t,x)}\,\mathrm{d}x\,, \\ -\partial_{xx}\phi^0 + c(t)\,e^{\phi^0(t,x)} = n_i(t,x)\,, & E^0 = -\partial_x\phi^0\,. \end{cases} \tag{4}$$

Remark 1. *Notice that t is only a parameter in this Limit-model, coming from the time-dependency of the ion density. Therefore, the value of f^0 at $t = 0$ could be* a priori *incompatible with the initial condition of the electron distribution function f^ε solution of the kinetic equation (1). We need thus to address subtly the question of the transition between the kinetic regime (1) and the macroscopic description (4) for an ill-prepared initial datum. This specific point of an initial layer is also addressed in Theorem 2.*

The identification and well-posedness of the non-linear elliptic L-model will be investigated in Section 3. In Section 4, the rigorous convergence of $(f^\varepsilon, E^\varepsilon)$, solution to (1), towards the solution (f^0, E^0) of the limit model (4), is done via hypocoercivity arguments, the latter being directly inspired by [1]. It is an analysis conducted in a perturbative context, and based on the linearization of the transport operator $v\,\partial_x - E^\varepsilon\,\partial_v$.

Theorem 2. ***(Asymptotic behaviour)*** *Let $(f^\varepsilon, E^\varepsilon)$ be a distributional solution of the nonlinear system (1), with a given ion density $n_i \in W^{1,\infty}((0,T);L^1(\mathbb{T}_x))$, such that $\int_{\mathbb{T}_x} n_i(t,x)\,\mathrm{d}x \equiv \mathfrak{m}$. Assume furthermore that $f^\varepsilon \in \mathcal{C}^0([0,T], L^2_\sigma(\mathbb{T}_x \times \mathbb{R}_v))$ and $E^\varepsilon = -\partial_x \phi^\varepsilon \in L^\infty((0,T)\times\mathbb{T}_x)$. There exists then a constant $\eta_0 > 0$ such that, if the initial condition of the perturbation is small enough, in the sense*

$$\|f^\varepsilon_{in} - n^0_{in}\mathcal{M}\|^2_{L^2_\sigma(\mathbb{T}_x\times\mathbb{R}_v)} \leqslant \eta_0, \qquad \forall \varepsilon > 0, \tag{5}$$

one finds constants $C_0, C_1, C_2, \varepsilon_0 > 0$ such that

$$\|f^\varepsilon(t) - n^0(t)\mathcal{M}\|^2_{L^2_\sigma(\mathbb{T}_x\times\mathbb{R}_v)} \leqslant C_0\|f^\varepsilon_{in} - n^0_{in}\mathcal{M}\|^2_{L^2_\sigma(\mathbb{T}_x\times\mathbb{R}_v)} e^{-\frac{C_1 t}{\varepsilon}} + C_2\varepsilon^2, \qquad \forall \varepsilon \leqslant \varepsilon_0, \forall t \in [0,T]. \tag{6}$$

This theorem permits to highlight the presence of an initial layer of size ε in time. In other terms, the influence of an ill-prepared initial condition vanishes exponentially in the variable t/ε. Furthermore, as we shall see in the proof (see Remark 7), the constant C_2 in this Theorem depends solely on the time derivative of the limit density $n^0(t,x) = c(t)e^{\phi^0}$ defined by (4). Therefore, C_2 is zero when n_i does not depend on time.

Estimate (6) allows also to find an explicit convergence rate towards the adiabatic regime, after integrating in time, namely

$$\|f^\varepsilon - n^0\mathcal{M}\|_{L^p((0,T);L^2_\sigma(\mathbb{T}_x\times\mathbb{R}_v))} \underset{\varepsilon\to 0}{=} \mathcal{O}(\varepsilon^{1/p}), \qquad \text{for all } p \in [1,+\infty[. \tag{7}$$

Notice that the term related to the dissipation of the initial layer $C_0\|f^\varepsilon_{in} - n^0_{in}\mathcal{M}\|^2_{L^2_\sigma(\mathbb{T}_x\times\mathbb{R}_v)} e^{-\frac{C_1 t}{\varepsilon}}$, is the dominant term. If we assume that the initial condition is well prepared in the sense

$$\|f^\varepsilon_{in} - n^0_{in}\mathcal{M}\|_{L^2_\sigma(\mathbb{T}_x\times\mathbb{R}_v)} = \mathcal{O}(\sqrt{\varepsilon}),$$

we will get an improved behaviour

$$\|f^\varepsilon - n^0\mathcal{M}\|_{L^p((0,T);L^2_\sigma(\mathbb{T}_x\times\mathbb{R}_v))} \underset{\varepsilon\to 0}{=} \mathcal{O}(\varepsilon^{2/p}), \qquad \text{for all } p \in [1,+\infty[. \tag{8}$$

This result will be proven in this paper in a Hermite spectral setting. One may wonder about the optimality of assumption (5). The reason for this assumption is the perturbative nature of our approach. In [1], the authors manage to avoid this assumption thanks to a convergence argument based on the $H-$theorem. In a context of a time-dependent ion density n_i, this latter approach however fails, and getting rid of assumption (5) remains an open question.

Estimate (6) of Theorem 2 permits also to evaluate the convergence rates of the Hermite modes, as summarized in the following Corollary.

Corollary 1. ***(Hermite coefficient behaviour)*** *Assume that the conditions of Theorem 2 are met. Then decomposing the particle distribution density f^ε in the Hermite basis via (3) yields*

$$\|C^\varepsilon_k\|_{L^2((0,T)\times\mathbb{T}_x)} = \mathcal{O}\left(\sqrt{\frac{\varepsilon}{k}}\right), \qquad \forall k \geqslant 1 \quad \textit{and} \quad \varepsilon \ll 1. \tag{9}$$

This is a first step towards an efficient numerical treatment of the adiabatic $\varepsilon \to 0$ regime of (1). The higher the index in the infinite hierarchy of Hermite coefficients, the smaller the importance of the coefficient. This estimate is not a pointwise-in-time estimate, but rather an L^2-result. Furthermore, the estimate in k is not sharp, as our analysis is conducted in a $L^2_\sigma(\mathbb{T}_x \times \mathbb{R}_v)$ setting . A way to get sharper results would be to carry out an analysis in a $H^s_\sigma(\mathbb{T}_x \times \mathbb{R}_v)$ setting, with a general $s \in \mathbb{R}$, as in [22]. This may be the object of future works.

Finally, in view of this estimate, and inspired by the numerical results of [14], we perform in the rest of this paper numerical simulations to confirm the mathematical results and investigate further the electron adiabatic asymptotics. Furthermore we adapt this scheme to cope with the singular limit $\varepsilon \to 0$, resulting in an *Asymptotic-Preserving* scheme.

1.2. **Outline of the paper.** The paper is organised as follows : in Section 2, we quickly state a result on the well-posedness of system (1) for fixed ε, and give some physical properties of (1). In Section 3 we identify formally the limit problem when $\varepsilon \to 0$ and prove some related existence, uniqueness and regularity results that will be useful in the rigorous treatment. Section 4 introduces the Hermite formalism we will work with, along with the functional spaces and operators and their respective properties. In subsection 4.3.1, in particular, we adapt the formalism of [1] to our time-dependent setting, and state the hypocoercivity properties that will lead to our Theorem 2. Theorem 2 is proven in Section 5, along with Corollary 1. Finally, in Section 6, numerical schemes are presented both for the computation of the kinetic problem (1), and of the limit problem (4). We validate the kinetic scheme thanks to the features of our Theorem 2. Numerical investigations aimed to highlight Corollary 1 are performed. Finally, in Section 7, we investigate the properties of this numerical scheme in the singular limit $\varepsilon \to 0$, considering a fixed mesh. Then we adjust it in such a way that the scheme becomes *Asymptotic-Preserving* and demonstrate numerically this last essential property. The paper finishes with some conclusions and open problems for future works.

2. The Kinetic Vlasov-Poisson-Fokker-Planck equation

Before starting with the asymptotic study, we shall firstly recall in this section some existence and uniqueness results about the Vlasov-Poisson-Fokker-Planck model (1), and state some properties of this equation as well of its solution.

2.1. **The kinetic model for fixed $\varepsilon > 0$.** Many authors have worked on the mathematical study of this type of Fokker-Planck equation for given electric force fields, showing the existence/uniqueness of strong/weak solutions, local/global in time. For the coupled, nonlinear Vlasov-Poisson-Fokker-Planck problem (1), see for ex. [11] for a global strong existence result in $2D_x2D_v$, or [5] where an existence result in the $3D_x3D_v$ setting is proven, assuming only the initial condition to be in $L^1 \cap L^\infty$, with finite moments of order 6.

The long-time behaviour of the solutions, in the case of a time-independent ion density is also well documented : see [6] for instance, for a method based on compactness techniques. More recently, [1] extends those results by giving an explicit convergence rate towards the long-time equilibrium, in a $L^2_\sigma(\mathbb{T}_x \times \mathbb{R}_v)$ setting and using hypocoercivity techniques. The long-time asymptotics in a $H^s_\sigma(\mathbb{T}_x \times \mathbb{R}_v)$ framework is studied in [22].

Our problem (1) is slightly different due to the presence of a time-dependent ion density and we state the following existence and uniqueness result based on bootstrap arguments, fixed point techniques, Duhamel formulations and short time regularizations (see [20, 21, 27, 33] for this last point) of the operator $P : \mathcal{D}(P) \subset L^2_\sigma(\mathbb{T}_x \times \mathbb{R}_v) \to L^2_\sigma(\mathbb{T}_x \times \mathbb{R}_v)$, $P := v\partial_x - \partial_v\,[v + \partial_v]$. One can check [20] for a proof of the following theorem, proof that adapts without any difficulty to our setting.

Theorem 3. ***(Existence and Uniqueness)*** *Let $\varepsilon > 0$ fixed, $n_i \in L^\infty((0,T); L^1(\mathbb{T}_x))$ and an initial condition $f^\varepsilon_{in} \in L^2_\sigma(\mathbb{T}_x \times \mathbb{R}_v)$. Then there exists a unique couple $(f^\varepsilon, E^\varepsilon)$ of mild solutions of (1), satisfying $f^\varepsilon \geqslant 0$ and*

- $f^\varepsilon \in \mathcal{C}^0([0,T], L^2_\sigma(\mathbb{T}_x \times \mathbb{R}_v))$,
- $E^\varepsilon \in L^\infty((0,T) \times \mathbb{T}_x)$.

A mild solution of (1) is a couple of functions $(f^\varepsilon, E^\varepsilon)$ satisfying

$$\begin{cases} f^\varepsilon(t) = f^\varepsilon_{in} + \dfrac{1}{\varepsilon}\displaystyle\int_0^t e^{-(t-s)P/\varepsilon}(\partial_v(E^\varepsilon f^\varepsilon)(s))\,\mathrm{d}s, \\ E^\varepsilon = -\partial_x\phi^\varepsilon, \qquad -\partial_{xx}\phi^\varepsilon = n_i - n^\varepsilon_e = n_i - \displaystyle\int_{\mathbb{R}_v} f^\varepsilon\,\mathrm{d}v, \end{cases}$$

where $e^{-tP/\varepsilon}$ is the semigroup generated by the operator P/ε.

Remark 2. *Notice that with this definition of a mild solution, f^ε is also a solution in the distributional sense, and one can show furthermore that $f^\varepsilon \in L^2((0,T)\times\mathbb{T}_x; H^1_\gamma(\mathbb{R}_v))$.*

Remark 3. *Let us remark also that ϕ^ε is unique up to an additive constant. How this constant shall be fixed is of no importance for the computation of the distribution function f^ε, however it has to be specified if one is interested in the computation of the potential.*

2.2. **The Fokker-Planck Operator.** For the study of the asymptotics of f^ε towards f^0 it is important to know more about the linear Fokker-Planck collision operator, given by

$$\mathcal{C} : D(\mathcal{C}) \subset L^2_\gamma(\mathbb{R}_v) \to L^2_\gamma(\mathbb{R}_v)\,, \qquad \mathcal{C}(f) := \partial_v\left[v\,f + \partial_v f\right] = \partial_v\left[\mathcal{M}\,\partial_v\left(\frac{f}{\mathcal{M}}\right)\right]\,, \tag{10}$$

with definition domain

$$D(\mathcal{C}) := \{f \in L^2_\gamma(\mathbb{R}_v) \;\;/\;\; \mathcal{C}(f) \in L^2_\gamma(\mathbb{R}_v)\}.$$

Remark that $\mathcal{C}$ acts only on the velocity variable, the time and space variables are considered as parameters. The following proposition summarizes now the properties of conservation and entropy decay, which are very easily proven using (10).

Proposition 1. *The Fokker-Planck collision operator $\mathcal{C}$ defined in (10) satisfies the following properties:*

- *Mass conservation:*
$$\int_{\mathbb{R}_v} \mathcal{C}(f)\,\mathrm{d}v = 0, \qquad \forall f \in D(\mathcal{C});$$
- *Entropy Decay:*
$$\int_{\mathbb{R}_v} \mathcal{C}(f)\ln(f/\mathcal{M})\,\mathrm{d}v \le 0, \qquad \forall f \in D(\mathcal{C}), \quad \mathcal{C}(f)\ln(f/\mathcal{M}) \in L^1(\mathbb{R}_v);$$
- *Thermal equilibrium:*
$$\int_{\mathbb{R}_v} \mathcal{C}(f)\ln(f/\mathcal{M})\,\mathrm{d}v = 0 \quad \Leftrightarrow \quad f(v) = n\,\mathcal{M}(v), \quad n \in \mathbb{R}\,,$$
$$\forall f \in D(\mathcal{C}), \quad \mathcal{C}(f)\ln(f/\mathcal{M}) \in L^1(\mathbb{R}_v).$$

Let us observe furthermore that this collision operator does not preserve momentum and energy.

2.3. **Macroscopic quantities and H-theorem.** We shall associate to the particle distribution function f^ε macroscopic quantities, like the particle density, the local current and the kinetic energy densities given respectively by

$$n^\varepsilon(t,x) := \int_{\mathbb{R}_v} f^\varepsilon(t,x,v)\;\mathrm{d}v\,, \qquad j^\varepsilon(t,x) := (n^\varepsilon u^\varepsilon)(t,x) = \int_{\mathbb{R}_v} v\,f^\varepsilon\;\mathrm{d}v\,,$$

$$w^\varepsilon(t,x) := \frac{1}{2}\int_{\mathbb{R}_v} v^2\,f^\varepsilon\;\mathrm{d}v\,.$$

Taking the moments of (1) one obtains the non-closed system of macroscopic conservation laws

$$\begin{cases} \partial_t n^\varepsilon + \dfrac{1}{\varepsilon}\,\partial_x j^\varepsilon = 0\,, \\ \partial_t j^\varepsilon + \dfrac{2}{\varepsilon}\,\partial_x w^\varepsilon + \dfrac{1}{\varepsilon}\,n^\varepsilon\,E^\varepsilon = -\dfrac{1}{\varepsilon}\,j^\varepsilon\,, \\ \partial_t w^\varepsilon + \dfrac{1}{2\varepsilon}\,\partial_x\langle v^3\,f^\varepsilon\rangle + \dfrac{1}{\varepsilon}\,j^\varepsilon\,E^\varepsilon = -\dfrac{2}{\varepsilon}\,w^\varepsilon + \dfrac{1}{\varepsilon}\,n^\varepsilon\,, \end{cases} \tag{11}$$

where we used the notation $\langle g\rangle := \int_{\mathbb{R}_v} g\,\mathrm{d}v$. To close the system one has to express the term $\langle v^3\,f^\varepsilon\rangle$ be means of the quantities $(n^\varepsilon, u^\varepsilon, w^\varepsilon)$. This can be done in the limit $\varepsilon \to 0$, leading to a fully well-posed macroscopic model.

The remaining part of this section is not necessary for the rest of this paper, is added however here for completeness, permitting a better understanding of the $\varepsilon \ll 1$ regime. The kinetic and potential energies corresponding to problem (1), are defined as

$$\mathcal{K}^\varepsilon(t) := \frac{1}{2}\int_{\mathbb{T}_x}\int_{\mathbb{R}_v} v^2\, f^\varepsilon(t,x,v)\ \mathrm{d}v\,\mathrm{d}x\,, \quad \mathcal{P}^\varepsilon(t) := \frac{1}{2}\int_{\mathbb{T}_x} |\partial_x\phi^\varepsilon(t,x)|^2\ \mathrm{d}x\,,$$

and the entropy is

$$\mathcal{H}^\varepsilon(t) := \int_{\mathbb{T}_x}\int_{\mathbb{R}_v} f^\varepsilon\ \ln(f^\varepsilon)\ \mathrm{d}v\,\mathrm{d}x\,.$$

Thus, the free-energy, which is the sum of the last three terms, is given then by

$$\mathcal{F}^\varepsilon(t) := \frac{1}{2}\int_{\mathbb{T}_x}\int_{\mathbb{R}_v} v^2\, f^\varepsilon\ \mathrm{d}v\,\mathrm{d}x + \frac{1}{2}\int_{\mathbb{T}_x} |\partial_x\phi^\varepsilon|^2\ \mathrm{d}x + \int_{\mathbb{T}_x}\int_{\mathbb{R}_v} f^\varepsilon\ \ln(f^\varepsilon)\ \mathrm{d}v\,\mathrm{d}x\,,$$

and the free-energy dissipation by

$$\mathcal{D}^\varepsilon(t) := \int_{\mathbb{T}_x}\int_{\mathbb{R}_v} \frac{1}{f^\varepsilon}\,|v\, f^\varepsilon + \partial_v f^\varepsilon|^2\ \mathrm{d}v\,\mathrm{d}x = 4\int_{\mathbb{T}_x}\int_{\mathbb{R}_v} \left|\partial_v\sqrt{f^\varepsilon/\mathcal{M}}\right|^2 \mathcal{M}\ \mathrm{d}v\,\mathrm{d}x\,.$$

The relative entropy will be denoted and defined by

$$\mathcal{H}(f/g) := \int_{\mathbb{T}_x}\int_{\mathbb{R}_v} (f\ \ln(f/g) - f + g)\ \mathrm{d}v\,\mathrm{d}x.$$

All of these quantities are connected through the so called H-Theorem.

Proposition 2. ***(H-Theorem)*** *Assume f^ε to be a strong, as smooth as desired, solution of (1), and assume that $n_i \in L^1(\mathbb{T}_x)$ is time-independent. Multiplying the Fokker-Planck equation with $\ln(f^\varepsilon/\mathcal{M})$ and integrating over the phase space (x,v), we obtain the evolution equation*

$$\frac{\mathrm{d}}{\mathrm{d}t}\mathcal{H}\left(f^\varepsilon/\mathcal{M}\right) + \frac{1}{2}\frac{\mathrm{d}}{\mathrm{d}t}\int_{\mathbb{T}_x} |\partial_x\phi^\varepsilon|^2\ \mathrm{d}x + \frac{1}{\varepsilon}\,\mathcal{D}^\varepsilon(t) = 0, \tag{12}$$

which yields, after integration in time

$$\varepsilon\,\mathcal{F}^\varepsilon(t) + \int_0^t \mathcal{D}^\varepsilon(s)\,ds = \varepsilon\,\mathcal{F}^\varepsilon(0)\,. \tag{13}$$

Equally, one can obtain the following relation

$$\frac{\mathrm{d}}{\mathrm{d}t}\mathcal{H}\left(\frac{f^\varepsilon}{n^0\,\mathcal{M}}\right) + \frac{1}{2}\frac{\mathrm{d}}{\mathrm{d}t}\int_{\mathbb{T}_x} |\partial_x\phi^\varepsilon(t,x) - \partial_x\phi^0(x)|^2\ \mathrm{d}x + \frac{4}{\varepsilon}\int_{\mathbb{T}_x}\int_{\mathbb{R}_v}\left|\partial_v\sqrt{\frac{f^\varepsilon}{\mathcal{M}}}\right|^2 \mathcal{M}\ \mathrm{d}v\,\mathrm{d}x = 0\,. \tag{14}$$

3. Formal Identification and Well-Posedness of the limit model

Let us investigate now formally the $\varepsilon \to 0$ limit of the kinetic model (1) in the aim to identify the asymptotic limit model. We shall prove Theorem 1, saying that if f^ε is a strong solution of (1), of mass $\mathfrak{m}$, then formally $f^\varepsilon \to f^0$, where f^0 is given by the limit model (4), which we remind here

$$(L)\quad \begin{cases} f^0(t,x,v) = c(t)\ e^{\phi^0(t,x)}\,\mathcal{M}(v)\,, \qquad c(t) = \dfrac{\mathfrak{m}}{\int_{\mathbb{T}_x} e^{\phi^0(t,x)}\,\mathrm{d}x}\,, \quad \mathfrak{m} := \displaystyle\int_{\mathbb{T}_x}\int_{\mathbb{R}_v} f^0_{in}(x,v)\ \mathrm{d}v\,\mathrm{d}x\,, \\ -\partial_{xx}\phi^0 + c(t)\,e^{\phi^0(t,x)} = n_i\,. \end{cases}$$

Proof of Theorem 1. To obtain the Limit-model, several steps are performed:

(a) H-theorem: Multiplying the kinetic equation (1) by $\ln(\frac{f^\varepsilon}{e^{\phi^\varepsilon}\,\mathcal{M}})$ and letting formally $\varepsilon \to 0$ permits to show that

$$\int_{\mathbb{T}_x}\int_{\mathbb{R}_v} \mathcal{C}(f^0)\ln\left(\frac{f^0}{e^{\phi^0}\,\mathcal{M}}\right)\mathrm{d}v\,\mathrm{d}x = \int_{\mathbb{T}_x}\int_{\mathbb{R}_v} \mathcal{C}(f^0)\ln(f^0/\mathcal{M})\,\mathrm{d}v\,\mathrm{d}x = 0\,,$$

yielding (see Proposition 1)

$$f^0(t,x,v) = n^0(t,x)\,\mathcal{M}\,, \qquad \forall (t,x) \in \mathbb{R}^+\times\mathbb{T}_x\,,$$

with $n^0(t,x)$ still to be determined.

(b) Struggle between transport and collision operator: If we make now use of the kinetic equation (1), we get at highest order in ε the equation

$$v\,\partial_x f^0 - E^0\,\partial_v f^0 = \mathcal{C}(f^0)\,.$$

Inserting the Maxwellian $f^0 = n^0(t,x)\,\mathcal{M}$ obtained in the first step into this last equation, yields

$$v\,\partial_x n^0\,\mathcal{M} - E^0\,n^0\,\partial_v\mathcal{M} = 0 \quad \Rightarrow \quad \partial_x n^0 - n^0\,\partial_x\phi^0 = 0\,,$$

permitting to get finally the Limit-model (4).

□

Thus it is the combination between the dissipative operator (H-theorem, step (a)) and the transport operator (step (b)) which permits to converge towards the Boltzmann equilibrium.

Remark 4. *Item (b) can be also replaced by a different strategy, the so called* moment method, *using the macroscopic equations* (11)*:*

(c) Show that in some sense $j^\varepsilon \underset{\varepsilon\to 0}{\to} j^0 = \int_{\mathbb{R}_v} v\,f^0\,\mathrm{d}v = 0$ *and* $w^\varepsilon \underset{\varepsilon\to 0}{\to} w^0 = \frac{1}{2}\int_{\mathbb{R}_v} v^2\,f^0\,\mathrm{d}v = n^0$*;*

(d) In the limit $\varepsilon \to 0$*, the second equation of* (11) *yields then formally*

$$\partial_x n^0 + n^0\,E^0 = 0\,.$$

The existence and uniqueness of a solution of the obtained limit-model (4) for a fixed ion density n_i is given in the following proposition.

Proposition 3. ***(Existence and uniqueness)*** *Let us fix the total electron mass* $\mathfrak{m} > 0$ *and furthermore assume that the ion density is known, satisfying* $n_i \in L^\infty(\mathbb{R}_+; L^1(\mathbb{T}_x))$ *and the constraint* $\int_{\mathbb{T}_x} n_i\,\mathrm{d}x = \mathfrak{m}$*. Then the non-linear elliptic problem*

$$-\partial_{xx}\phi^0 + c(t)\,e^{\phi^0(t,x)} = n_i\,, \tag{15}$$

associated with the intrinsic solvability condition

$$c(t)\int_{\mathbb{T}_x} e^{\phi^0(t,x)}\,\mathrm{d}x = \mathfrak{m}\,, \tag{16}$$

periodic boundary conditions in $x \in \mathbb{T}_x$ *and the additional constraint*

$$\int_{\mathbb{T}_x} \phi^0(t,x)\,\mathrm{d}x = 0\,, \tag{17}$$

admits a unique solution $\phi^0 \in L^\infty(\mathbb{R}_+; H^1(\mathbb{T}_x))$*. Furthermore, thanks to* (15) *one has even*

$$\partial_x\phi^0 \in L^\infty(\mathbb{R}_+, W^{1,1}(\mathbb{T}_x)) \subset L^\infty(\mathbb{R}_+\times\mathbb{T}_x).$$

If the data are more regular in space, in particular for $n_i \in L^\infty(\mathbb{R}_+; L^2(\mathbb{T}_x))$ *one gets more regular solutions, namely* $\phi^0 \in L^\infty(\mathbb{R}_+; H^2(\mathbb{T}_x))$*.*

Proof. Let us start by considering firstly the time $t \in \mathbb{R}_+$ as a parameter and let us introduce the space $\mathcal{H} := \{g \in H^1(\mathbb{T}_x)\ /\ \int_{\mathbb{T}_x} g(x)\,\mathrm{d}x = 0\}$. The proof is then divided in three steps.

1. Step: Existence/uniqueness for fixed $t \in \mathbb{R}_+$*.*
Standard elliptic theory permits to show the existence and uniqueness of a solution $\phi^0(t) \in \mathcal{H}$ to the equation (15)-(17). This is based on the minimization of the strictly convexe, Gateaux differentiable functional on the space $\mathcal{H}$

$$\mathcal{L}(\phi) := \frac{1}{2}\int_{\mathbb{T}_x} |\partial_x\phi|^2\,\mathrm{d}x + \mathfrak{m}\,\ln\left(\int_{\mathbb{T}_x} e^\phi\,\mathrm{d}x\right) - \int_{\mathbb{T}_x} n_i\,\phi\,\mathrm{d}x\,.$$

Remark that one has the compact injection $H^1(\mathbb{T}_x) \subset C(\mathbb{T}_x)$.

2. Step: Regularity in time.
The regularity in time comes now from the fact that t is only a parameter in (15). Indeed, multiplying this equation with $\phi^0 \in \mathcal{H}$ and integrating in space, yields

$$||\partial_x \phi^0||^2_{L^2(\mathbb{T}_x)}(t) + \mathfrak{m} \int_{\mathbb{T}_x} e^{\phi^0(t,x)}\, \phi^0(t,x)\, \mathrm{d}x = \int_{\mathbb{T}_x} n_i\, \phi^0(t,x)\, \mathrm{d}x\,,$$

leading, via Poincaré's inequality and with some time-independent constants $\alpha, \beta > 0$, to

$$\begin{aligned}
\alpha||\phi^0||^2_{H^1(\mathbb{T}_x)}(t) + \mathfrak{m} \int_{\phi^0>0} e^{\phi^0(t,x)}\, \phi^0(t,x)\, \mathrm{d}x &\leqslant ||n_i||_{L^1(\mathbb{T}_x)}\, ||\phi^0(t)||_{L^\infty(\mathbb{T}_x)} \\
&\quad -\mathfrak{m} \textstyle\int_{\phi^0<0} e^{\phi^0(t,x)}\, \phi^0(t,x)\, \mathrm{d}x \\
&\leqslant ||n_i||_{L^1(\mathbb{T}_x)}\, ||\phi^0(t)||_{L^\infty(\mathbb{T}_x)} + \mathfrak{m}\, ||\phi^0(t)||_{L^1(\mathbb{T}_x)} \\
&\leqslant \beta ||\phi^0(t)||_{H^1(\mathbb{T}_x)}\,.
\end{aligned}$$

Thus one has $||\phi^0(t)||_{H^1(\mathbb{T}_x)} \leqslant \beta/\alpha$ for all $t \geqslant 0$.

3. Step: Regularity in space.
For more regular data, namely if $n_i \in L^\infty((0,T); L^2(\mathbb{T}_x))$ one gets immediately from the equation (15) that $\phi^0 \in L^\infty(\mathbb{R}_+; H^2(\mathbb{T}_x))$, for all $t \in \mathbb{R}_+$. □

We therefore have an existence result for the Limit problem (15), associated with the constraint (17). This constraint was comfortable to work with when dealing with existence and uniqueness, but for the proof of Theorem 2, it is more convenient to use the following constraint (18), namely

$$\int_{\mathbb{T}_x} e^{\phi^0(t,y)}\, \mathrm{d}y \equiv 1\,. \tag{18}$$

Notice that if ϕ^0 satisfies (15) to (17), then $\phi^0 - \ln\left(\int_{\mathbb{T}_x} e^{\phi^0}\, \mathrm{d}x\right)$ satisfies (15),(16) and (18).

We shall now give a further time-regularity result for the solution of the limit problem with this constraint (18).

Proposition 4. ***(Further time regularity)*** *Assume further $n_i \in W^{1,\infty}((0,T); L^1(\mathbb{T}_x))$, with $\int_{\mathbb{T}_x} n_i(t,x)\, \mathrm{d}x \equiv \mathfrak{m}$ and denote by ϕ^0 the solution of (15)-(16) associated with the different constraint (18), namely*

$$\int_{\mathbb{T}_x} e^{\phi^0(t,y)}\, \mathrm{d}y \equiv 1\,.$$

Then the solution actually has the regularity $\phi^0 \in W^{1,\infty}((0,T); H^1(\mathbb{T}_x))$. One can further show that

$$\partial_t \phi^0 \in L^\infty((0,T); W^{1,\infty}(\mathbb{T}_x)).$$

Proof. This proposition is proven by derivating in the weak sense equation (15) : $\partial_t \phi^0$ is the solution of the following linear elliptic problem in g

$$\begin{cases} -\partial_{xx} g + \mathfrak{m} g\, e^{\phi^0(t,x)} = \partial_t n_i, \\ \displaystyle\int_{\mathbb{T}_x} g(t,x)\, e^{\phi^0(t,x)}\, \mathrm{d}x \equiv 0. \end{cases}$$

Standard elliptic arguments permit to conclude that this problem admits a unique solution $g = \partial_t \phi^0 \in L^\infty((0,T); H^1(\mathbb{T}_x))$. Using again the equation permits to have further $\partial_{xx} g \in L^\infty((0,T); L^1(\mathbb{T}_x))$ and hence $\partial_t \phi^0 \in L^\infty((0,T); W^{1,\infty}(\mathbb{T}_x))$. □

4. Rigorous asymptotic via hypocoercivity arguments

In this section we shall treat rigorously the $\varepsilon \to 0$ asymptotic limit of the Vlasov-Poisson-Fokker-Planck system (1) with initial condition $f_{in}^\varepsilon \in L^2_\sigma(\mathbb{T}_x \times \mathbb{R}_v)$ and a given time-dependent ion density $n_i \in W^{1,\infty}((0,T); L^1(\mathbb{T}_x))$. This shall be done using hypocoercivity arguments. Let us begin by recalling our starting kinetic problem

$$(V)_\varepsilon \quad \begin{cases} \partial_t f^\varepsilon + \dfrac{1}{\varepsilon}\, v\, \partial_x f^\varepsilon - \dfrac{1}{\varepsilon}\, E^\varepsilon\, \partial_v f^\varepsilon = \dfrac{1}{\varepsilon}\partial_v \left[v\, f^\varepsilon + \partial_v f^\varepsilon \right] , \\ -\partial_{xx}\phi^\varepsilon = n_i - n^\varepsilon, \qquad E^\varepsilon = -\partial_x \phi^\varepsilon \,, \qquad n^\varepsilon = \displaystyle\int_{\mathbb{R}_v} f^\varepsilon(t,x,v)\, \mathrm{d}v \,, \\ f^\varepsilon(t=0,x,v) = f_{in}^\varepsilon(x,v) \,, \end{cases}$$

which admits (Theorem 3) for each $\varepsilon > 0$ a unique mild solution $(f^\varepsilon, E^\varepsilon)$ verifying

- $f^\varepsilon \in \mathcal{C}^0([0,T], L^2_\sigma(\mathbb{T}_x \times \mathbb{R}_v)) \cap L^2((0,T) \times \mathbb{T}_x, H^1_\gamma(\mathbb{R}_v))$,
- $E^\varepsilon = -\partial_x \phi^\varepsilon \in L^\infty((0,T) \times \mathbb{T}_x)$.

The corresponding nonlinear elliptic limit problem (15)-(16), with the additional constraint (18) to fix ϕ^0

$$(L) \quad \begin{cases} n^0(t,x) = \mathfrak{m}\, e^{\phi^0(t,x)} \,, \\ -\partial_{xx}\phi^0 = n_i - n^0 \,, \\ \displaystyle\int_{\mathbb{T}_x} e^{\phi^0(t,x)}\, \mathrm{d}x \equiv 1 \,, \end{cases} \tag{19}$$

has (Proposition 4) a unique solution $\phi^0 \in W^{1,\infty}((0,T); H^1(\mathbb{T}_x))$, such that $\partial_t \phi^0 \in L^\infty((0,T); W^{1,\infty}(\mathbb{T}_x))$. The $\varepsilon \to 0$ asymptotic study will be performed in a Hermite spectral formalism we shall define now.

4.1. The Hermite spectral formalism.

Let us start by expanding the electron distribution function $f^\varepsilon(t,x,v)$ as follows

$$f^\varepsilon(t,x,v) = \sum_{k=0}^\infty C_k^\varepsilon(t,x)\, \psi_k(v) \,, \quad f_{in}(x,v) = \sum_{k=0}^\infty C_{k,in}(x) \psi_k(v) \,, \tag{20}$$

where $\{\psi_k\}_{k\in\mathbb{N}}$ are Hermite functions defined recursively as

$$\sqrt{k+1}\, \psi_{k+1}(v) = v\, \psi_k(v) - \sqrt{k}\, \psi_{k-1} \,, \qquad \psi_{-1} \equiv 0 \,, \;\; \psi_0 \equiv \mathcal{M} \,, \;\; \psi_1 \equiv v\, \mathcal{M} \,, \tag{21}$$

and which satisfy

$$\psi_k'(v) = -\sqrt{k+1}\, \psi_{k+1}(v) \,, \qquad \int_{-\infty}^\infty \psi_k(v)\, \psi_l(v)\, \mathrm{d}\gamma(v) = \delta_{kl} \,, \quad \forall k,l \in \mathbb{N} \,.$$

These Hermite functions form a complete, orthonormal basis of $L^2_\gamma(\mathbb{R}_v)$. System (1) therefore rewrites as an infinite hierarchy of nonlinear, coupled PDEs

$$\begin{cases} \varepsilon\, \partial_t C_k^\varepsilon(t,x) + \sqrt{k}\, \partial_x C_{k-1}^\varepsilon - \sqrt{k}\, \partial_x \phi^\varepsilon(t,x)\, C_{k-1}^\varepsilon + \sqrt{k+1}\, \partial_x\, C_{k+1}^\varepsilon + k\, C_k^\varepsilon = 0 \,, \quad \forall k \in \mathbb{N}, \\ -\partial_{xx}\phi^\varepsilon = n_i - C_0^\varepsilon, \\ C_k^\varepsilon(t=0,\cdot) = C_{k,in}, \end{cases} \tag{22}$$

where we set $C_{-1}^\varepsilon := 0$. Remark that the Fokker-Planck collision operator becomes now in the Hermite-framework a simple multiplication operator.

We shall prove in the next sections the $\varepsilon \to 0$ convergence of the distribution function f^ε towards the limit problem (19) by using this Hermite-approach and showing that in some sense

$$\left\{ \begin{array}{lll} C_0^\varepsilon & \to_{\varepsilon\to 0} & n^0, \\ C_k^\varepsilon & \to_{\varepsilon\to 0} & 0, \\ \partial_x \phi^\varepsilon & \to_{\varepsilon\to 0} & \partial_x \phi^0, \end{array} \right. \qquad \forall k \in \mathbb{N}^*,$$

where the quantities (n^0, ϕ^0) are solutions of (19).

4.2. **Filtering of the equilibrium.** Our strategy is to use a perturbative approach, based on the decomposition $f^\varepsilon = \underbrace{n^0(t,x)\mathcal{M}(v)}_{\text{asymptotic regime}} + \underbrace{g^\varepsilon}_{\text{fluctuation}}$ which reformulates, in Hermite variables, as

$$f^\varepsilon(t,x,v) = \sum_{k=0}^{\infty} C_k^\varepsilon(t,x)\psi_k(v), \qquad g^\varepsilon(t,x,v) = \sum_{k=0}^{\infty} \gamma_k^\varepsilon(t,x)\psi_k(v),$$

with

$$\left\{ \begin{array}{rcll} C_0^\varepsilon &=& n^0 + \gamma_0^\varepsilon, & \\ C_k^\varepsilon &=& 0 + \gamma_k^\varepsilon, & \forall k \in \mathbb{N}^*, \\ \phi^\varepsilon &=& \phi^0 + \varphi^\varepsilon, & \end{array} \right.$$

and we want to show that these new variables $(\{\gamma_k^\varepsilon\}_{k\in\mathbb{N}}, \varphi^\varepsilon)$ converge to zero in a way that we shall specify later. The decomposition in asymptotic and fluctuating part leads to the following set of equations for the fluctuating Hermite variables $(\{\gamma_k^\varepsilon\}_{k\in\mathbb{N}}, \varphi^\varepsilon)$

$$\left\{ \begin{array}{l} \varepsilon\, \partial_t \gamma_0^\varepsilon + \partial_x \gamma_1^\varepsilon = -\varepsilon \partial_t n^0, \\ \varepsilon\, \partial_t \gamma_1^\varepsilon + \partial_x \gamma_0^\varepsilon - \partial_x \phi^0 \gamma_0^\varepsilon + \sqrt{2}\partial_x \gamma_2^\varepsilon - \partial_x \varphi^\varepsilon n^0 + \gamma_1^\varepsilon = \partial_x \varphi^\varepsilon \gamma_0^\varepsilon, \\ \varepsilon\, \partial_t \gamma_k^\varepsilon + \sqrt{k}\, \partial_x \gamma_{k-1}^\varepsilon - \sqrt{k}\, \partial_x \phi^0 \gamma_{k-1}^\varepsilon + \sqrt{k+1}\, \partial_x \gamma_{k+1}^\varepsilon + k\gamma_k^\varepsilon = \sqrt{k}\partial_x \varphi^\varepsilon \gamma_{k-1}^\varepsilon, \quad \forall k \geqslant 2 \\ -\partial_{xx}\varphi^\varepsilon = -\gamma_0^\varepsilon, \end{array} \right. \tag{23}$$

where we used that the limiting density verifies $\partial_x n^0 = \partial_x \phi^0 n^0$. In the following, the fluctuation variable vector $\{\gamma_k^\varepsilon\}_{k\in\mathbb{N}}$ will be simply denoted by γ^ε and we shall fix the fluctuating potential by imposing $\int_{\mathbb{T}_x} \varphi^\varepsilon \, \mathrm{d}x = 0$.

Remark 5. *Notice that integrating with respect to $x \in \mathbb{T}_x$ the relation $C_0^\varepsilon = n^0 + \gamma_0^\varepsilon$ yields the constraint*

$$\int_{\mathbb{T}_x} \gamma_0^\varepsilon(t,x)\, \mathrm{d}x = 0, \quad \forall t \in [0,T].$$

This remark, along with the functional space to which f^ε belongs, invites to define the following Hilbert spaces for the fluctuating Hermite-coefficient vector γ^ε

$$l_0^2(\mathbb{N}, L^2(\mathbb{T}_x)) := \left\{ \gamma \in l^2(\mathbb{N}, L^2(\mathbb{T}_x)) \;\Big/\; \int_{\mathbb{T}_x} \gamma_0(x)\, \mathrm{d}x = 0 \right\},$$

$$h_0^1(\mathbb{N}, L^2(\mathbb{T}_x)) := \left\{ \gamma \in l_0^2(\mathbb{N}, L^2(\mathbb{T}_x)) \;\Big/\; \sum_k k \|\gamma_k\|^2_{L^2(\mathbb{T}_x)} < \infty \right\}.$$

Therefore for

$$f^\varepsilon \in \mathcal{C}^0([0,T], L^2_\sigma(\mathbb{T}_x \times \mathbb{R}_v)) \cap L^2((0,T)\times \mathbb{T}_x; H^1_\gamma(\mathbb{R}_v)),$$

and $\phi^0 \in W^{1,\infty}((0,T); H^1(\mathbb{T}_x))$, we have the following regularity of the fluctuation variable

$$\gamma^\varepsilon \in \mathcal{C}^0([0,T], l_0^2(\mathbb{N}, L^2(\mathbb{T}_x))) \cap L^2((0,T), h_0^1(\mathbb{N}, L^2(\mathbb{T}_x))).$$

Let us introduce now some notation enabling to write system (23) in a more concise way, namely

$$\varepsilon\,\partial_t\gamma^\varepsilon + \mathcal{T}_t\gamma^\varepsilon - \mathcal{L}\gamma^\varepsilon = \varepsilon\,\mathcal{S} + \mathcal{Q}[\gamma^\varepsilon], \tag{24}$$

where for smooth $\alpha = \{\alpha_k\}_{k\in\mathbb{N}} \in l^2_0(\mathbb{N}, L^2(\mathbb{T}_x))$ the time-dependent *linearized* transport operator is defined (for given (n^0, ϕ^0)) as

$$\mathcal{T}_t\alpha := \begin{bmatrix} \partial_x\alpha_1 & & & & & & \\ \partial_x\alpha_0 & - & \partial_x\phi^0(t,\cdot)\alpha_0 & + & \sqrt{2}\,\partial_x\alpha_2 & - & \partial_x\varphi_\alpha n^0(t,\cdot) \\ \sqrt{2}\,\partial_x\alpha_1 & - & \sqrt{2}\,\partial_x\phi^0(t,\cdot)\alpha_1 & + & \sqrt{3}\,\partial_x\alpha_3 & & \\ & & & \vdots & & & \\ \sqrt{k}\,\partial_x\alpha_{k-1} & - & \sqrt{k}\,\partial_x\phi^0(t,\cdot)\alpha_{k-1} & + & \sqrt{k+1}\,\partial_x\alpha_{k+1} & & \\ & & & \vdots & & & \end{bmatrix}, \tag{25}$$

with domain $\mathcal{D}(\mathcal{T}_t) := \{\alpha \in l^2_0(\mathbb{N}, L^2(\mathbb{T}_x)),\ \mathcal{T}_t\alpha \in l^2_0(\mathbb{N}, L^2(\mathbb{T}_x))\}$ and φ_α computed via

$$-\partial_{xx}\varphi_\alpha = -\alpha_0\,, \qquad \int_{\mathbb{T}_x}\varphi_\alpha\,\mathrm{d}x = 0\,.$$

The linear Fokker-Planck collision operator $\mathcal{L}$ has the simple form

$$\mathcal{L}\alpha := [0, -\alpha_1, \cdots, -k\alpha_k, \cdots]^t, \tag{26}$$

with domain $\mathcal{D}(\mathcal{L}) = h^2(\mathbb{N}, L^2(\mathbb{T}_x)) := \{\alpha \in l^2(\mathbb{N}, L^2(\mathbb{T}_x)),\ \sum_k k^2\|\alpha_k\|^2_{L^2(\mathbb{T}_x)} < \infty\}$.

The source term $\mathcal{S}$ contains terms coming from the time-dependence of the density

$$\mathcal{S}(t,x) := [-\partial_t n^0(t,x), 0, \cdots]^t\,,$$

and $\mathcal{Q}$ is the term regrouping all the "small" quadratic fluctuation terms

$$\mathcal{Q}[\alpha] := \left[0,\ \partial_x\varphi_\alpha\alpha_0,\ \ldots,\ \sqrt{k}\,\partial_x\varphi_\alpha\alpha_{k-1}\ \ldots\right]^t.$$

Finally, in order to distinguish between the macroscopic part and the mesoscopic part of the distribution function, we define the following projection operator

$$\Pi\alpha := [\alpha_0, 0, \cdots]^t, \quad \text{and} \quad (\mathbb{I}\mathrm{d} - \Pi)\alpha := [0, \alpha_1, \cdots, \alpha_k, \cdots]^t, \tag{27}$$

where $\Pi : l^2(\mathbb{N}, L^2(\mathbb{T}_x)) \to \ker\mathcal{L}$ is the orthogonal projection on the set of local equilibria of the Fokker-Planck operator.

4.3. **The functional space and its properties.** The aim of this subsection is to introduce all the necessary ingredients required to prove our main theorem, in particular the functional spaces, functional inequalities *etc.* Let us consider the time-dependent measure defined on $\mathbb{T}_x$ by $\mathrm{d}\eta_t(x) = (n^0(t,x))^{-1}\mathrm{d}x$ and the space $L^2_{\eta_t}(\mathbb{T}_x)$, which is nothing but the $L^2(\mathbb{T}_x)$-space endowed with the slightly different Hilbert scalar-product, given for fixed $t \in [0,T]$ and $a, b \in L^2(\mathbb{T}_x)$ by

$$\langle a, b\rangle_{L^2_{\eta_t}(\mathbb{T}_x)} := \int_{\mathbb{T}_x} a(x)b(x)\,\mathrm{d}\eta_t(x).$$

We will work in this paper with the space $l^2(\mathbb{N}, L^2_{\eta_t}(\mathbb{T}_x))$. This last choice of space is actually the same as in [1], however with the difference that we are using the Hermite spectral formalism for the velocity variable, and a time-dependent setting. Adapting their work, let us use the following time-dependent norm on the closed subspace $l^2_0(\mathbb{N}, L^2_{\eta_t}(\mathbb{T}_x)) := \{\alpha \in l^2(\mathbb{N}, L^2_{\eta_t}(\mathbb{T}_x)), \int_{\mathbb{T}_x}\alpha_0\,\mathrm{d}x \equiv 0\}$

$$\|\alpha\|^2_t := \sum_{k=0}^{\infty}\|\alpha_k\|^2_{L^2_{\eta_t}(\mathbb{T}_x)} + \int_{\mathbb{T}_x}(\partial_x\varphi_\alpha)^2\,\mathrm{d}x, \tag{28}$$

where $-\partial_{xx}\varphi_\alpha = -\alpha_0$ defines φ_α through the constraint $\int_{\mathbb{T}_x}\varphi_\alpha\,\mathrm{d}x = 0$. We are thus incorporating a nonlocal term in our norm. We denote by $\langle\cdot,\cdot\rangle_t$ the associated time-dependent scalar product.

We will furthermore make use of the adjoint operator and the orthogonal to a functional space X. These notions depend on t, but since we will never consider simultaneously two times, we just denote them as usual by $*$ and $X^\perp$ and without ambiguity.

In the following proposition, we shall regroup the properties of $l^2_0(\mathbb{N}, L^2_{\eta_t}(\mathbb{T}_x))$ endowed with the $\|\cdot\|_t$ norm.

Proposition 5. ***($\|\cdot\|_t$ norm)***

(1) The space $L^2_{\eta_t}(\mathbb{T}_x)$ is uniformly in t equivalent to $L^2(\mathbb{T}_x)$, more specifically, there exist time-independent constants $c, C > 0$ such that

$$c\|h\|^2_{L^2(\mathbb{T}_x)} \leqslant \|h\|^2_{L^2_{\eta_t}(\mathbb{T}_x)} \leqslant C\|h\|^2_{L^2(\mathbb{T}_x)}, \qquad \forall h \in L^2(\mathbb{T}_x), \quad \forall t \in [0,T].$$

(2) There exist furthermore time-independent constants $c, C > 0$ such that we have the norm equivalence

$$c\|\alpha\|^2_{l^2(\mathbb{N},L^2(\mathbb{T}_x))} \leqslant \|\alpha\|^2_t \leqslant C\|\alpha\|^2_{l^2(\mathbb{N},L^2(\mathbb{T}_x))}, \qquad \forall \alpha \in l^2_0(\mathbb{N}, L^2(\mathbb{T}_x)), \quad \forall t \in [0,T].$$

(3) $\mathcal{T}_t$ is skew-symmetric, namely

$$\langle \mathcal{T}_t\alpha, \alpha\rangle_t = 0, \qquad \forall \alpha \in \mathcal{D}(\mathcal{T}_t), \quad \forall t \in [0,T].$$

(4) Π is symmetric, i.e.

$$\langle \Pi\alpha, \beta\rangle_t = \langle \alpha, \Pi\beta\rangle_t, \qquad \forall \alpha, \beta \in l^2(\mathbb{N}, L^2(\mathbb{T}_x), \quad \forall t \in [0,T].$$

Proof. The first point is a result of the fact that $\phi^0 \in L^\infty((0,T)\times\mathbb{T}_x)$. The second point is due to the the first point, and the following sequence of inequalities, obtained from the classical Poincaré-Wirtinger inequality

$$0 \leqslant \int_{\mathbb{T}_x} (\partial_x\varphi_\alpha)^2 \,\mathrm{d}x \leqslant \kappa \int_{\mathbb{T}_x} (\alpha_0)^2 \,\mathrm{d}x \leqslant \kappa\, \|n^0\|_\infty \|\alpha_0\|^2_{L^2_{\eta_t}(\mathbb{T}_x)}.$$

For the third point, we compute

$$\begin{aligned}
\langle \mathcal{T}_t\alpha, \alpha\rangle_t =& \sum_{k=0}^{\infty} \langle \sqrt{k+1}\,\partial_x\alpha_{k+1} + \sqrt{k}\,\partial_x\alpha_{k-1} - \sqrt{k}\,\partial_x\phi^0(t,\cdot)\alpha_{k-1}, \alpha_k\rangle_{L^2_{\eta_t}(\mathbb{T}_x)} \\
&+ \underbrace{\int_{\mathbb{T}_x} \partial_x\varphi_{\mathcal{T}_t\alpha}\partial_x\varphi_\alpha \,\mathrm{d}x}_{\text{non-local part of the scalar product}} \underbrace{- \langle \partial_x\varphi_\alpha n^0, \alpha_1\rangle_{L^2_{\eta_t}(\mathbb{T}_x)}}_{\text{additional term of k=1}} \\
&= \sum_{k=0}^{\infty} \langle \sqrt{k+1}\,\partial_x\alpha_{k+1} + \sqrt{k}\,\partial_x\alpha_{k-1} - \sqrt{k}\,\partial_x\phi^0(t,\cdot)\alpha_{k-1}, \alpha_k\rangle_{L^2_{\eta_t}(\mathbb{T}_x)} \\
&+ \int_{\mathbb{T}_x} \partial_x\varphi_{\mathcal{T}_t\alpha}\partial_x\varphi_\alpha \,\mathrm{d}x - \int_{\mathbb{T}_x} \partial_x\varphi_\alpha\alpha_1 \,\mathrm{d}x.
\end{aligned}$$

The first term in this equality sums to zero, because of an integration by parts and a telescopic sum, and the two other terms cancel out, because of an integration by parts and the fact that $\partial_{xx}\varphi_{\mathcal{T}_t\alpha} = (\mathcal{T}_t\alpha)_0 = \partial_x\alpha_1$. The fourth point is straightforward. □

Remark 6. *To simplify the notation and due to the equivalence property of Proposition 5 (1) and (2), we shall denote in the following simply by $L^2(\mathbb{T}_x)$ the space $L^2_{\eta_t}(\mathbb{T}_x)$ endowed with the norm (28).*

Proposition 6. ***(The linear Fokker-Planck operator)*** *The linear Fokker-Planck operator $\mathcal{L} : \mathcal{D}(\mathcal{L}) = h^2(\mathbb{N}, L^2(\mathbb{T}_x)) \to l^2(\mathbb{N}, L^2(\mathbb{T}_x))$ satisfies the following properties*

(1) $\mathcal{L}$ can be extended to an operator

$$\tilde{\mathcal{L}} : h^1(\mathbb{N}, L^2(\mathbb{T}_x)) \to h^{-1}(\mathbb{N}, L^2(\mathbb{T}_x)) := \left\{ \{\alpha_k\}_{k\in\mathbb{N}} \in L^2(\mathbb{T}_x)^{\mathbb{N}} \;\Big/\; \sum_{k>1} \frac{1}{k} \|\alpha_k\|^2_{L^2(\mathbb{T}_x)} < \infty \right\}.$$

(2) $\mathcal{L}$ is self-adjoint, namely, $\mathcal{D}(\mathcal{L}) = \mathcal{D}(\mathcal{L}^*)$, and

$$\langle \mathcal{L}\alpha, \beta\rangle_t = \langle \alpha, \mathcal{L}\beta\rangle_t, \qquad \forall \alpha, \beta \in \mathcal{D}(\mathcal{L}), \quad \forall t \in [0,T].$$

(3) $\mathcal{L}$ is a closed operator, and we have that

$$\mathrm{Im}\, \mathcal{L} = (\ker \mathcal{L})^\perp = (\ker \tilde{\mathcal{L}})^\perp = \{\alpha \in l^2(\mathbb{N}, L^2(\mathbb{T}_x)) \;/\; \alpha_0 = 0\}.$$

*(4) **Microscopic coercivity :** The operator $-\mathcal{L}$ is coercive on $(\ker \mathcal{L})^\perp \cap \mathcal{D}(\mathcal{L})$, namely*

$$-\langle \mathcal{L}\alpha, \alpha\rangle_t \geqslant \|(\mathbb{I}d - \Pi)\alpha\|^2_t, \qquad \forall t \in [0,T], \quad \forall \alpha \in h^2(\mathbb{N}, L^2(\mathbb{T}_x)). \tag{29}$$

The Microscopic coercivity property (29) expresses the fact that the collision operator relaxes the electron density towards a local Maxwellian distribution function belonging to the kernel of $\mathcal{L}$. We only prove the fourth point, as the first three ones are immediate from the definition of $\mathcal{L}$ and its expression in terms of the Hermite coefficients (26).

Proof of (4). The micro-coercivity property is the reformulation of the following inequality

$$\sum_{k=1}^{\infty} k \|\alpha_k\|^2_{L^2_{\eta_t}(\mathbb{T}_x)} \geqslant \sum_{k=1}^{\infty} \|\alpha_k\|^2_{L^2_{\eta_t}(\mathbb{T}_x)},$$

where we keep in mind that $\varphi_{\mathcal{L}\alpha} = 0$. The conclusion follows from Pareseval's theorem. □

Now that we have introduced the notations and explicited some properties of the functional space, we are ready to move to the next subsection, dealing with hypocoercivity and aimed to be a toolbox that we will use in Section 6.

4.3.1. *Hypocoercivity toolbox.* Entropy methods are strategies for proving the exponential decay of solutions of evolution equations of the type

$$\begin{cases} \partial_t u + \mathcal{B} u = 0\,, \\ u(t=0,\cdot) = u_0\,, \end{cases} \tag{30}$$

towards the equilibrium solution u_{eq} satisfying $\mathcal{B} u_{eq} = 0$. The main idea is to find a suitable entropy functional (Lyapunov functional) in terms of the considered operator $\mathcal{B}$ and equivalent to the underlying Hilbert-norm, permitting to measure the decay towards the equilibrium. For ex. to find a scalar-product $\langle\cdot,\cdot\rangle_{\mathcal{B}}$, equivalent to the underlying scalar-product, however for which $\mathcal{B}$ is coercive, meaning

$$\langle \mathcal{B}\, u, u\rangle_{\mathcal{B}} \geqslant \lambda ||u||^2_{\mathcal{B}}\,, \quad \forall u \in D(\mathcal{B}) \cap (\ker \mathcal{B})^\perp\,,$$

such that one obtains from (30)

$$\frac{1}{2}\frac{\mathrm{d}}{\mathrm{d}t} ||u||^2_{\mathcal{B}} = \langle \partial_t u, u\rangle_{\mathcal{B}} \leqslant -\lambda ||u||^2_{\mathcal{B}}\,,$$

leading with Gronwall's lemma to the desired exponential decay

$$||u(t)||^2_{\mathcal{B}} \leqslant e^{-2\,\lambda\, t}\, ||u_0||^2_{\mathcal{B}}\,, \qquad \forall t \geqslant 0\,.$$

In order to prove Theorem 2, namely the exponential decay of f^ε in the t/ε variable, towards the asymptotic regime $n^0\mathcal{M}$, we shall investigate the convergence towards zero of the fluctuations, solutions of the Hermite system

$$\varepsilon\, \partial_t \gamma^\varepsilon + \mathcal{T}_t \gamma^\varepsilon - \mathcal{L}\gamma^\varepsilon = \varepsilon\, \mathcal{S} + \mathcal{Q}[\gamma^\varepsilon], \tag{31}$$

trying to find a suitable functional $\mathcal{F}_t$, which is equivalent to the norm $\|\cdot\|_t$ (uniformly in time) and which satisfies moreover an inequality of the form

$$\frac{\mathrm{d}}{\mathrm{d}t}\mathcal{F}_t(\gamma^\varepsilon) \leqslant \mathcal{G}_\varepsilon\left(\mathcal{F}_t(\gamma^\varepsilon)\right), \tag{32}$$

with $\mathcal{G}_\varepsilon$ a certain non-linear function.

Unfortunately the operator $\mathcal{T}_t - \mathcal{L}$ is not coercive for the $\|\cdot\|_t$ norm, we rather have for α smooth enough

$$\langle(\mathcal{T}_t - \mathcal{L})\alpha, \alpha\rangle_t \geqslant \|(\mathbb{I}\mathrm{d} - \Pi)\alpha\|_t^2. \tag{33}$$

This fact is due to both, the skew-symmetry of the transport operator and the microscopic coercivity of $\mathcal{L}$, which is coercive only on $(\ker \mathcal{L}_{|l_0^2(\mathbb{N},L^2(\mathbb{T}_x))})^\perp$, and not on the whole space. However, from the formal analysis performed in Section 3, we observed that the operator $\mathcal{T}_t - \mathcal{L}$ relaxes nevertheless the macroscopic part $\Pi\alpha$ towards zero, so that we can still expect an inequality of the form (32).

The problem is that the transport operator, skew-symmetric, is absent from the computations, while its mixing properties are essential to get an exponential decay in this $\|\cdot\|_t$ norm. This problematic has been widely called *hypocoercivity*.

There are several ways to introduce the effect of $\mathcal{T}_t$ to get the desired exponential decay for the hypocoercive operator $\mathcal{T}_t - \mathcal{L}$. Inspired by [1], we choose the so-called *auxiliary operator method*. The idea of this method is to add a well-chosen correction operator A_t to the standard entropy functional, and hence instead of working with the usual $\|\cdot\|_t$ norm, to work with the modified functional

$$\mathcal{F}_t(\gamma^\varepsilon(t)) := \frac{1}{2}\|\gamma^\varepsilon\|_t^2 + \delta\,\langle A_t\gamma^\varepsilon, \gamma^\varepsilon\rangle_t, \tag{34}$$

with $\delta > 0$ to be tuned later on. This functional will be designed in such a manner to be a Lyapunov functional for (31), and furthermore equivalent to the $\|\cdot\|_t$ norm. The operator A_t shall incorporate somehow the role of the transport operator $\mathcal{T}_t$.

The choice of the operator A_t is inspired by the Drift-Diffusion limit [1] and is defined by

$$A_t := (\mathbb{I}\mathrm{d} + (\mathcal{T}_t\Pi)^*(\mathcal{T}_t\Pi))^{-1}(\mathcal{T}_t\Pi)^*,$$

where the adjoint operator $*$ is, for fixed t, the adjoint operator corresponding to the Hilbertian scalar-product $\langle\cdot,\cdot\rangle_t$. The role of the operator A_t in the modified entropy (34) is similar to the mixing term $\langle\nabla_x\xi, \nabla_v\xi\rangle$ (see [21]), which, as the name suggests, permits to mix the two space and velocity variables in order to recover the missing space derivatives in the coercivity inequality (33).

The well-posedness of this operator

$$A_t : l_0^2(\mathbb{N}, L^2(\mathbb{T}_x)) \to l_0^2(\mathbb{N}, L^2(\mathbb{T}_x))$$

is a consequence of Lax-Milgram theorem, as stated in the next Proposition. In the next subsections some essential properties of this operator A_t will be summarized, being the basis for showing an estimate of the type (32).

4.3.2. *Properties of the mixing operator A_t.* The first inequality we shall introduce can be seen as the coercivity of the operator $(\mathcal{T}_t)^*\mathcal{T}_t$ on the space $\ker\mathcal{L} \cap \mathcal{D}((\mathcal{T}_t)^*\mathcal{T}_t)$.

Proposition 7. ***(Macroscopic coercivity)*** *Let $\mathcal{T}_t$ be the transport operator defined in (25). There exists a constant $\lambda_M > 0$ such that*

$$\|\mathcal{T}_t\Pi\alpha\|_t^2 \geqslant \lambda_M\|\Pi\alpha\|_t^2, \qquad \forall t \in [0,T], \quad \forall\alpha \in l_0^2(\mathbb{N}, H^1(\mathbb{T}_x)). \tag{35}$$

This uniform in time spectral gap inequality leads to the well-definitness of the operator A_t, and furthermore, to the coercivity of $A_t\mathcal{T}_t\Pi$ on $l^2_0(\mathbb{N}, L^2(\mathbb{T}_x))$, namely

$$\langle A_t\mathcal{T}_t\Pi\alpha, \alpha\rangle_t \geqslant \frac{\lambda_M}{1+\lambda_M}\|\Pi\alpha\|_t^2, \qquad \forall t\in[0,T], \quad \forall \alpha \in l^2_0(\mathbb{N}, L^2(\mathbb{T}_x)). \tag{36}$$

Proof. This property is based exclusively on the ideas of [1], with the specificity of the uniform-in-time Poincaré inequality given in Lemma 5, and also on Lax-Milgram theorem. Let us make here some further comments. The first inequality is a spectral gap inequality, indicating a uniform in time lower bound on the first eigenvalue of the positive operator $(\mathcal{T}_t\Pi)^*\mathcal{T}_t\Pi$. The second inequality is a consequence of the first one: since $A_t\mathcal{T}_t\Pi$ is just the composition of $z\mapsto z(1+z)^{-1}$ with the operator $(\mathcal{T}_t\Pi)^*(\mathcal{T}_t\Pi)$, diagonalizing this operator $(\mathcal{T}_t\Pi)^*(\mathcal{T}_t\Pi)$ leads to the second point. □

Decomposing now the space $l^2_0(\mathbb{N}, L^2(\mathbb{T}_x))$ as

$$l^2_0(\mathbb{N}, L^2(\mathbb{T}_x)) = \ker \mathcal{L}_{|l^2_0(\mathbb{N}, L^2(\mathbb{T}_x))} \oplus (\ker \mathcal{L}_{|l^2_0(\mathbb{N}, L^2(\mathbb{T}_x))})^\perp,$$

we see that the microscopic coercivity (29) guarantees a coercivity of the operator $\mathcal{T}_t - \mathcal{L}$ on $(\ker \mathcal{L}_{|l^2_0(\mathbb{N}, L^2(\mathbb{T}_x))})^\perp$, which is the reason of the relaxation towards zero on this space, whereas on the subspace $\ker\mathcal{L}$, the reason of relaxation towards zero will be the transport operator, and more explicitly, the macroscopic coercivity property (36) of the operator $\mathcal{T}_t^*\mathcal{T}_t$.

Now, the computation of $\varepsilon\frac{\mathrm{d}}{\mathrm{d}t}\mathcal{F}_t(\gamma^\varepsilon)$ will lead on one hand to the appearance of the microscopic and macroscopic coercivities, but on the other hand also to many other terms, that need to be controlled. We will detail the properties used to bound all these terms in the rest of this subsection. Some of these properties are identical to those introduced in [1] and will hence not be proven here.

Observing that we have

$$\mathcal{T}_t\Pi\alpha = \begin{bmatrix} 0 \\ \partial_x\alpha_0 - \partial_x\phi^0(t,\cdot)\alpha_0 - \partial_x\varphi_\alpha n^0(t,\cdot) \\ 0 \\ \vdots \end{bmatrix},$$

yields immediately the so-called *parabolic dynamics property* $\Pi\mathcal{T}_t\Pi = 0$, which implies, as in [12], the following Lemma.

Lemma 1. *[12] **(Parabolic macroscopic dynamics)** Let $\alpha\in l^2_0(\mathbb{N}, L^2(\mathbb{T}_x))$. First we observe that $\Pi A_t = A_t$, which leads to*

$$\|A_t\alpha\|_t^2 + \|T_tA_t\alpha\|_t^2 = \langle\alpha, \mathcal{T}_tA_t\alpha\rangle_t\,, \tag{37}$$

and then to

$$\|A_t\alpha\|_t \leqslant \frac{1}{2}\|(\mathbb{I}d-\Pi)\alpha\|_t, \quad \forall t\in[0,T]. \tag{38}$$

We deduce that $A_t = A_t(\mathbb{I}d-\Pi)$ and

$$\|T_tA_t\alpha\|_t \leqslant \|(\mathbb{I}d-\Pi)\alpha\|_t, \quad \forall t\in[0,T]. \tag{39}$$

For the remaining terms we have the following Lemma.

Lemma 2. ***(Bounded auxiliary operators)** Set $\alpha\in l^2_0(\mathbb{N}, L^2(\mathbb{T}_x))$. The auxiliary operator A_t has a regularising effect, namely we have*

$$\|A_t\mathcal{L}\alpha\|_t \leqslant \frac{1}{2}\|(\mathbb{I}d-\Pi)\alpha\|_t, \quad \forall t\in[0,T], \tag{40}$$

and $\exists\Lambda>0$ independent on time, such that

$$\|A_t\mathcal{T}_t(\mathbb{I}d-\Pi)\alpha\|_t \leqslant \Lambda\,\|(\mathbb{I}d-\Pi)\alpha\|_t, \quad \forall t\in[0,T]. \tag{41}$$

Proof. The proof of inequality (40) is exactly as in [1]. The proof of (41) is quite technical, but follows the lines of [1], Lemma 20, and is mainly based on integration by parts and the use of Poincaré type inequalities. A difference between [1] and our result is the time-independence of the constant Λ that needs to be addressed. This is assured because of our uniform in time Poincaré inequalities (see Lemma 5). The beginning of the proof follows exactly step 1 and 2 of [1]. However, keeping in mind that in our case n^0, $\partial_x\phi^0 \in L^\infty((0,T)\times\mathbb{T}_x)$ permits to greatly simplify the proof, as we do not need the estimates of their step 3. Their inequalities (32)-(33) of step 4 are a direct consequence of their inequalities (27)-(28). □

Now, because of the time dependency of the weight, as opposed to [1], there are some additional terms appearing in our computations. We show in the following Lemma that these additional terms can be properly handled.

Lemma 3. ***(Specificities due to the time-dependency of*** n_i***)*** *The commutator* $[\partial_t, A_t] := \partial_t A_t - A_t\partial_t$ *is uniformly bounded, namely*

$$\|[\partial_t, A_t]\alpha\|_t \leqslant C_*\|(\mathbb{I}d - \Pi)\alpha\|_t, \quad \forall t\in[0,T], \quad \forall \alpha \in L^\infty((0,T), l^2_0(\mathbb{N}, L^2(\mathbb{T}_x))), \tag{42}$$

with $C_* > 0$ *a time-independent constant, depending only on the* L^∞*-norm of* $\partial_t\partial_x\phi^0$, $\partial_t\phi^0$, *and* ϕ^0.

Proof. We prove this lemma in the Appendix. □

With these properties in mind, we are ready to deal with the proof of Theorem 2.

5. Proofs of Theorem 2 and Corollary 1

Let us come now to the rigorous asymptotic study of our nonlinear Vlasov-Poisson-Fokker-Planck system (1). Recalling that we decomposed f^ε in a macroscopic asymptotic part, and a fluctuation part $f^\varepsilon = n^0(t,x)\mathcal{M}(v) + g^\varepsilon$, with $g^\varepsilon = \sum_{k=0}^\infty \gamma_k^\varepsilon(t,x)\psi_k(v)$, we shall focus on the fluctuation problem

$$\varepsilon\,\partial_t\gamma^\varepsilon + \mathcal{T}_t\gamma^\varepsilon = \mathcal{L}\gamma^\varepsilon + \varepsilon\,\mathcal{S} + \mathcal{Q}[\gamma^\varepsilon].$$

Reformulating Theorem 2 with our new notation, we need to show that there exists $\eta_0 > 0$ such that, if the initial condition for the perturbation γ^ε_{in} is small enough, namely if

$$\|\gamma^\varepsilon_{in}\|^2_{l^2(\mathbb{N},L^2(\mathbb{T}_x))} = \|f^\varepsilon_{in} - n^0_{in}\mathcal{M}\|^2_{L^2_\sigma(\mathbb{T}_x\times\mathbb{R}_v)} \leqslant \eta_0, \qquad \forall\varepsilon>0\,,$$

we have the existence of constants $C_0, C_1, C_2, \varepsilon_0 > 0$ such that

$$\|f^\varepsilon(t) - n_0(t)\mathcal{M}\|^2_{L^2_\sigma(\mathbb{T}_x\times\mathbb{R}_v)} = \|\gamma^\varepsilon(t)\|^2_{l^2(\mathbb{N},L^2(\mathbb{T}_x))} \leqslant C_0\|\gamma^\varepsilon_{in}\|^2_{l^2(\mathbb{N},L^2(\mathbb{T}_x))}e^{-\frac{C_1 t}{\varepsilon}} + C_2\varepsilon^2, \quad \forall\varepsilon\leqslant\varepsilon_0,\ \forall t\in[0,T].$$

Proof of Theorem 2 : The proof is based on the study of the following entropy functional

$$\mathcal{F}_t(\gamma^\varepsilon(t)) := \frac{1}{2}\|\gamma^\varepsilon\|^2_t + \delta\,\langle A_t\gamma^\varepsilon, \gamma^\varepsilon\rangle_t\,, \tag{43}$$

introduced in Section 4.3.1. Notice that this functional $\mathcal{F}_t$ is equivalent to $\|\cdot\|^2_t$, uniformly in t, provided that $\delta > 0$ is small enough, i.e. one has, thanks to (38) and to the definition (27)

$$\frac{1}{2}(1-\delta)\|\cdot\|^2_t \leqslant \mathcal{F}_t \leqslant \frac{1}{2}(1+\delta)\|\cdot\|^2_t, \quad \forall t\in[0,T].$$

In the first part of the proof, using the tools of Section 4.3.1, we shall show the estimate

$$\varepsilon\frac{\mathrm{d}}{\mathrm{d}t}\mathcal{F}_t(\gamma^\varepsilon) \leqslant -\eta\mathcal{F}_t(\gamma^\varepsilon) + \varepsilon^2\,C_1 + C_2\mathcal{F}_t(\gamma^\varepsilon)^2, \tag{44}$$

which will lead, in a second time, to the convergence result, thanks to the smallness of the initial condition (5), Gronwall's Lemma and the equivalence with the $\|\cdot\|^2_t$ norm.

5.1. **Part 1 : Estimate obtention.** Derivating in time the entropy functional $\mathcal{F}_t$ (43), yields

$$\begin{aligned}
\varepsilon \frac{\mathrm{d}}{\mathrm{d}t}\mathcal{F}_t(\gamma^\varepsilon) =& \langle \mathcal{L}\gamma^\varepsilon, \gamma^\varepsilon\rangle_t - \delta\langle A_t\mathcal{T}_t\Pi\gamma^\varepsilon, \gamma^\varepsilon\rangle_t && \text{('Good dissipative terms')}\\
&- \delta\left\langle A_t\mathcal{T}_t(\mathbb{I}\mathrm{d}-\Pi)\gamma^\varepsilon, \gamma^\varepsilon\right\rangle_t + \delta\left\langle \mathcal{T}_tA_t\gamma^\varepsilon, \gamma^\varepsilon\right\rangle_t + \delta\left\langle A_t\mathcal{L}\gamma^\varepsilon, \gamma^\varepsilon\right\rangle_t + \delta\underbrace{\langle \mathcal{L}A_t\gamma^\varepsilon, \gamma^\varepsilon\rangle_t}_{=0}\\
&&& \text{(Signless terms arising in the classical computation)}\\
&+ \varepsilon\left\langle \mathcal{S}, \gamma^\varepsilon\right\rangle_t + \varepsilon\delta\underbrace{\langle A_t\mathcal{S}, \gamma^\varepsilon\rangle_t}_{=0} + \varepsilon\delta\left\langle A_t\gamma^\varepsilon, \mathcal{S}\right\rangle_t && \text{(Terms associated with the source term)}\\
&- \frac{\varepsilon}{2}\sum_{k=0}^{\infty}\langle \partial_t\phi^0\gamma_k^\varepsilon, \gamma_k^\varepsilon\rangle_{L^2_{\eta_t}(\mathbb{T}_x)} - \varepsilon\delta\sum_{k=0}^{\infty}\langle \partial_t\phi^0(A_t\gamma^\varepsilon)_k, \gamma_k^\varepsilon\rangle_{L^2_{\eta_t}(\mathbb{T}_x)} + \varepsilon\delta\left\langle [\partial_t, A_t]\gamma^\varepsilon, \gamma^\varepsilon\right\rangle_t\\
&&& \text{(Terms related to the time dependency of the norms and operators)}\\
&+ \left\langle \mathcal{Q}[\gamma^\varepsilon], \gamma^\varepsilon\right\rangle_t + \delta\left\langle A_t\mathcal{Q}[\gamma^\varepsilon], \gamma^\varepsilon\right\rangle_t + \delta\underbrace{\langle A_t\gamma^\varepsilon, \mathcal{Q}[\gamma^\varepsilon]\rangle_t}_{=0}.\\
&&& \text{(Terms arising due to the nonlinearity } \mathcal{Q})
\end{aligned} \tag{45}$$

Some terms vanish to zero due to $\mathcal{L}(A_t) = \mathcal{L}(\Pi A_t) = 0$, $A_t\mathcal{S} = A_t(\mathbb{I}\mathrm{d}-\Pi)\mathcal{S} = 0$ and $A_t = \Pi A_t$, which gives $\langle A_t\gamma^\varepsilon, \mathcal{Q}[\gamma^\varepsilon]\rangle_t = 0$.

The first line regroups the dissipation terms, which behave nicely because of the microscopic and macroscopic coercivities. We use estimates identical to the ones occuring in [1, 12], to control the terms of the second line by the microscopic and macroscopic coercivity. We compiled them in the Appendix, for the sake of completeness, inequalities (71) to (76). We also need to deal with the terms related to the source term and to the time dependency of the norms, gathered in the Appendix (inequality (77) to (82)) as they are essentially based on Young's inequality and Lemma 3.

There only remains to control the terms in the last line of (45), appearing because of the nonlinear coupling, and this will be detailed now.

5.1.1. ***Control of the terms arising because of the nonlinearity.*** We deal with the quadratic term $\mathcal{Q}[\gamma^\varepsilon]$ in the following way: the first term of the last line of (45) is controlled by the following sequence of inequalities

$$\begin{aligned}
\langle \mathcal{Q}[\gamma^\varepsilon], \gamma^\varepsilon\rangle_t &= \sum_{k=1}^{\infty}\sqrt{k}\left\langle \partial_x\varphi_\gamma^\varepsilon\cdot\gamma_{k-1}^\varepsilon, \gamma_k^\varepsilon\right\rangle_{L^2_{\eta_t}(\mathbb{T}_x)}\\
&\leqslant \frac{1}{2}\sum_{k=1}^{\infty}k\|\gamma_k^\varepsilon\|^2_{L^2_{\eta_t}(\mathbb{T}_x)} + \frac{1}{2}\sum_{k=0}^{\infty}\|\partial_x\varphi_\gamma^\varepsilon\gamma_k^\varepsilon\|^2_{L^2_{\eta_t}(\mathbb{T}_x)}\\
&\leqslant -\frac{1}{2}\langle \mathcal{L}\gamma^\varepsilon, \gamma^\varepsilon\rangle_t + \frac{\kappa}{2}\|\gamma^\varepsilon\|_t^4.
\end{aligned} \tag{46}$$

The passage from the second line to the third one uses the following sequence of inequalities, coming from the continuous Sobolev injection $H^1(\mathbb{T}_x) \hookrightarrow L^\infty(\mathbb{T}_x)$ and from the definition of the $\|\cdot\|_t$

$$\frac{1}{2}\sum_{k=0}^{\infty}\|\partial_x\varphi_\gamma^\varepsilon\gamma_k^\varepsilon\|^2_{L^2_{\eta_t}(\mathbb{T}_x)} \leqslant \frac{1}{2}\|\partial_x\varphi_\gamma^\varepsilon(t)\|^2_{L^\infty(\mathbb{T}_x)}\sum_{k=0}^{\infty}\|\gamma_k^\varepsilon\|^2_{L^2_{\eta_t}(\mathbb{T}_x)} \leqslant \frac{\kappa}{2}\|\gamma^\varepsilon\|_t^4.$$

The second term of the last line of (45) is controlled as follows, using (40)

$$\begin{aligned}\delta\langle A_t\mathcal{Q}[\gamma^\varepsilon],\gamma^\varepsilon\rangle_t &= \delta\langle A_t\mathcal{L}\mathcal{L}^{-1}\mathcal{Q}[\gamma^\varepsilon],\gamma^\varepsilon\rangle_t\\ &\leqslant \delta\|A_t\mathcal{L}\mathcal{L}^{-1}\mathcal{Q}[\gamma^\varepsilon]\|_t\|\gamma^\varepsilon\|_t\\ &\leqslant \frac{\delta}{2}\|\mathcal{L}^{-1}\mathcal{Q}[\gamma^\varepsilon]\|_t\|\gamma^\varepsilon\|_t\\ &\leqslant \frac{\delta}{2}\sqrt{\sum_{k=1}^{\infty}\left\|\frac{\sqrt{k}}{k}\partial_x\varphi^\varepsilon_\gamma.\gamma^\varepsilon_{k-1}\right\|^2_{L^2_{\eta_t}(\mathbb{T}_x)}}\|\gamma^\varepsilon\|_t \leqslant \frac{\delta\,\nu_5\,\kappa}{4}\|\gamma^\varepsilon\|_t^4+\frac{\delta}{4\nu_5}\|\gamma^\varepsilon\|_t^2\,, \end{aligned}\tag{47}$$

where $\nu_5>0$ will be adequately fixed later on. Notice that $\mathcal{L}^{-1}\mathcal{Q}$ is well defined, since $\Pi\mathcal{Q}=0$.

5.1.2. ***Summarizing the previous estimates.*** Assembling and reorganizing the terms of (45) and using all the estimates obtained so far, leads to

$$\begin{aligned}\varepsilon\frac{\mathrm{d}}{\mathrm{d}t}\mathcal{F}_t(\gamma^\varepsilon) \leqslant{}& \delta\left(\frac{1}{2\nu_1}+\frac{1}{2\nu_2}+\frac{1}{2\nu_3}-\frac{\lambda_M}{1+\lambda_M}\right)\|\Pi\gamma^\varepsilon\|_t^2 && \text{(Dissipation of } \Pi\gamma)\\ &+\left(\delta\Lambda^2\,\frac{\nu_1}{2}+\delta\frac{5}{4}+\delta\frac{\nu_2}{8}+\delta\frac{1}{8\nu_4}-\frac{1}{2}\right)\|(1-\Pi)\gamma^\varepsilon\|_t^2 && \text{(Dissipation of } (\mathbb{I}\mathrm{d}-\Pi)\gamma)\\ &+\frac{\varepsilon^2}{2}\left(\frac{\nu_3}{\delta}+\delta\nu_4\right)\|\mathcal{S}\|_t^2 && \text{(Source term)}\\ &+\varepsilon\,C_{\delta,\phi}\,\|\gamma^\varepsilon\|_t^2 && \text{(Time dependency)}\\ &+\kappa\left(\frac{1}{2}+\frac{\delta\nu_5}{4}\right)\|\gamma^\varepsilon\|_t^4+\frac{\delta}{4\nu_5}\|\gamma^\varepsilon\|_t^2, && \text{(Nonlinearity } \mathcal{Q})\end{aligned}$$

where $C_{\delta,\phi}:=\left(\frac{\|\partial_t\phi^0\|_\infty}{2}+\frac{\delta}{2}\|\partial_t\phi^0\|_\infty+\delta C_*\right)$ and $\nu_1,\nu_2,\nu_3,\nu_4,\nu_5>0$ are some constants to be tuned later on.

Choosing firstly ν_1, ν_2, $\nu_3>0$ such that the first line becomes strictly negative, tuning then $\delta>0$ and $\nu_4>0$ in order to get a strictly negative second line, permits to obtain the existence of an $\eta>0$ such that

$$\varepsilon\frac{\mathrm{d}}{\mathrm{d}t}\mathcal{F}_t(\gamma^\varepsilon)\leqslant-(\eta-\frac{\delta}{4\nu_5}-\varepsilon\,C_{\delta,\phi})\,\|\gamma^\varepsilon\|_t^2+\frac{\varepsilon^2}{2}\left(\frac{\nu_3}{\delta}+\delta\nu_4\right)\|\mathcal{S}\|_t^2+\kappa\left(\frac{1}{2}+\frac{\delta\nu_5}{4}\right)\|\gamma^\varepsilon\|_t^4.$$

Taking now $0<\eta_1<\eta$ and a small $\varepsilon_0>0$, and choosing furthermore $\nu_5>0$ big enough, depending on η, yields the existence of constants C', $C''>0$ such that

$$\varepsilon\frac{\mathrm{d}}{\mathrm{d}t}\mathcal{F}_t(\gamma^\varepsilon)\leqslant-\eta_1\,\|\gamma^\varepsilon\|_t^2+\varepsilon^2C'+C''\,\|\gamma^\varepsilon\|_t^4,\quad\forall t\in[0,T],\quad\forall\varepsilon<\varepsilon_0.\tag{48}$$

Remark 7. *Notice that the constant C' depends solely on the source term $\mathcal{S}$, which is zero when the density n_i is time-independent.*

Using the equivalence between $\mathcal{F}_t$ and $\|\cdot\|_t^2$, estimate (48) rewrites, up to changing the names of the constants, as

$$\frac{\mathrm{d}}{\mathrm{d}t}\mathcal{F}_t(\gamma^\varepsilon)\leqslant-\frac{\eta}{\varepsilon}\mathcal{F}_t(\gamma^\varepsilon)+\varepsilon\,C_1+\frac{C_2}{\varepsilon}\mathcal{F}_t(\gamma^\varepsilon)^2=\frac{\mathcal{F}_t(\gamma^\varepsilon)}{\varepsilon}(C_2\mathcal{F}_t(\gamma^\varepsilon)-\eta)+\varepsilon\,C_1.\tag{49}$$

We now want to conclude by Gronwall's lemma, but we need to be cautious, because of the quadratic term, and this is precisely where we will use the assumption on the smallness of the initial condition.

5.2. **Part 2 : Gronwall's Lemma with smallness of the initial condition.**

If the initial condition is too big, the quadratic term in (49) is bigger than the linear term, and $\mathcal{F}_t$ can explode in finite time. If, however the initial condition is very small, the first term on the right-hand side of (49) is negative, and the functional remains controlled. We write this rigorously in the following Lemma.

Lemma 4. *Assume that there exists constants η, C_1, $C_2 > 0$ such that the function $t \in [0,T] \to \mathcal{F}_t(\gamma^\varepsilon)$ verifies inequality (49). Assume now that $\mathcal{F}_0(\gamma^\varepsilon_{in}) \leqslant \frac{\eta}{2C_2}$. Then if $\varepsilon_1 > 0$ is such that $\varepsilon_1 C_1 \leqslant \frac{\eta}{8C_2T}$, we have*

$$\mathcal{F}_t(\gamma^\varepsilon) \leqslant \frac{3}{4}\frac{\eta}{C_2}\,, \qquad \forall \varepsilon < \varepsilon_1,\ \ \forall t \in [0,T]\,.$$

Proof. We are going to prove the following intermediate result

$$\mathcal{F}_t(\gamma^\varepsilon) \leqslant \frac{\eta}{2C_2} + \frac{t\eta}{4TC_2}\,, \qquad \forall \varepsilon < \varepsilon_1,\ \ \forall t \in [0,T]\,,$$

which implies immediately the Lemma. To do this, we fix $\varepsilon < \varepsilon_1$, and define

$$E := \left\{ t \in [0,T] \ \ / \ \ \mathcal{F}_s(\gamma^\varepsilon(s)) \leqslant \frac{\eta}{2C_2} + \frac{s\eta}{4TC_2} \quad \forall s \in [0,t] \right\}.$$

Let us prove that $\sup E = T$. Firstly, this set is nonempty, because of the smallness of the initial condition, which imposes $0 \in E$. Furthermore, because of Gronwall's Lemma applied to inequality (49), we will prove *by contradiction* that $\sup E = T$.

Assume indeed that $\sup E = t^* < T$. Then, using (49) for $t = t^*$, and the following inequality

$$\mathcal{F}_{t^*}(\gamma^\varepsilon) \leqslant \frac{\eta}{2C_2} + \frac{t^*\eta}{4TC_2} \leqslant \frac{3}{4}\frac{\eta}{C_2},$$

gives

$$\frac{\mathrm{d}}{\mathrm{d}t}\mathcal{F}_t(\gamma^\varepsilon)_{|t=t^*} \leqslant \frac{\mathcal{F}_{t^*}(\gamma^\varepsilon)}{\varepsilon}(C_2\mathcal{F}_{t^*}(\gamma^\varepsilon) - \eta) + \varepsilon\, C_1 \leqslant -\frac{\eta\,\mathcal{F}_{t^*}(\gamma^\varepsilon)}{4\varepsilon} + \varepsilon\, C_1.$$

We then use the assumption $\varepsilon_1 C_1 \leqslant \frac{\eta}{8C_2T}$, to get that

$$\frac{\mathrm{d}}{\mathrm{d}t}\mathcal{F}_t(\gamma^\varepsilon)_{|t=t^*} \leqslant \frac{\eta}{8C_2T}.$$

Using the definition of the derivative at time t^* gives that $\sup E > t^*$, which is a contradiction. □

Now let us assume that we have the smallness condition (5) on the initial condition, with η_0 so small that $\mathcal{F}_0(\gamma^\varepsilon_{in}) \leqslant \frac{\eta}{2C_2}$ holds. The conditions of the previous lemma are thus satisfied and the estimate (49) rewrites now

$$\frac{\mathrm{d}}{\mathrm{d}t}\mathcal{F}_t(\gamma^\varepsilon) \leqslant \frac{\mathcal{F}_t(\gamma^\varepsilon)}{\varepsilon}(C_2\mathcal{F}_t(\gamma^\varepsilon) - \eta) + \varepsilon\, C_1 \leqslant -\frac{\eta}{4}\frac{\mathcal{F}_t(\gamma^\varepsilon)}{\varepsilon} + \varepsilon\, C_1.$$

The result follows, using Gronwall's Lemma and the equivalence between $\|\cdot\|_{l^2(\mathbb{N},L^2(\mathbb{T}_x))}$ and $\sqrt{\mathcal{F}_t}$, along with Parseval's theorem. □

We conclude this section with the proof of Corollary 1.

Proof of Corollary 1. Taking the scalar-product of (31) with γ^ε yields

$$\begin{aligned}\varepsilon\,\frac{\mathrm{d}}{\mathrm{d}t}\|\gamma^\varepsilon\|_t^2 - \langle \mathcal{L}\gamma^\varepsilon, \gamma^\varepsilon\rangle_t &= \varepsilon\,\langle \mathcal{S}, \gamma^\varepsilon\rangle_t - \frac{\varepsilon}{2}\sum_{k=0}^{\infty}\langle \partial_t\phi^0\gamma^\varepsilon_k, \gamma^\varepsilon_k\rangle_{L^2_{\eta_t}(\mathbb{T}_x)} + \langle \mathcal{Q}[\gamma^\varepsilon], \gamma^\varepsilon\rangle_t \\ &\leqslant \frac{\varepsilon^2}{2}\,\|\mathcal{S}\|_t^2 + \left(\frac{1}{2} + \frac{\varepsilon}{2}\,\|\partial_t\phi^0\|_\infty\right)\,\|\gamma^\varepsilon\|_t^2 + \langle \mathcal{Q}[\gamma^\varepsilon], \gamma^\varepsilon\rangle_t.\end{aligned}$$

Using the bound (46) for the quadratic term and integrating in time over $[0,T]$, implies

$$\varepsilon\,\|\gamma^\varepsilon\|_T^2+\frac{1}{2}\int_0^T\langle-\mathcal{L}\gamma^\varepsilon(s),\,\gamma^\varepsilon(s)\rangle_s\,\mathrm{d}s\leqslant\varepsilon^2\sup_{s\in[0,T]}\|\mathcal{S}\|_s^2+\int_0^T C(\|\gamma^\varepsilon(s)\|_s^2+\|\gamma^\varepsilon(s)\|_s^4)\,\mathrm{d}s$$
$$\leqslant c_1\,\varepsilon^2+c_2\,\varepsilon,$$

where we injected the result of Theorem 2 to pass from the first line to the second one. The control of the second term of the left-hand side gives the desired result, thanks to Parseval's equality. □

6. Numerical investigations

In the rest of this paper we shall be concerned with the introduction of a performant numerical scheme for the resolution of the kinetic problem (1). In this aim, we firstly present a Newton strategy to compute the solution of the limit problem (4). Then a Hermite-Fourier spectral approach is proposed for the resolution of the kinetic equation (1). And finally, we use these schemes to investigate further the mathematical results obtained in the previous parts.

6.1. Numerical Scheme for the Limit problem.

In this subsection we present the methodology chosen to discretize the limit problem (4), called Poisson-Boltzmann model, task which is not so trivial due to the occurrence of the exponential term. Our numerical scheme is an iterative method based on Newton's procedure.

In more details, the nonlinear elliptic limit problem (4) for the electric potential ϕ^* reads

$$-\partial_{xx}\phi^*+\mathfrak{m}\frac{e^{\phi^*(t,x)}}{\displaystyle\int_{\mathbb{T}_x}e^{\phi^*(t,y)}\,\mathrm{d}y}=n_i(t,x),\qquad\forall x\in\mathbb{T}_x\,,\tag{50}$$

associated with periodic boundary conditions in x and where $t\in[0,T]$ is a fixed parameter. Given ϕ^*, the corresponding limiting electron density is given by Boltzmann's relation $n^*(t,x)=\mathfrak{m}\frac{e^{\phi^*(t,x)}}{\int_{\mathbb{T}_x}e^{\phi^*(t,y)}\,\mathrm{d}y}$. Notice that the solution ϕ^* of (50) is uniquely defined up to an additive constant, we shall fix by imposing $\int_{\mathbb{T}_x}\phi^*(t,x)\,\mathrm{d}x\equiv 0$. In the aim to solve (50), the first idea could be a naive fixed point strategy of the following form : given ϕ^j, compute the next iteration ϕ^{j+1} via

$$-\partial_{xx}\phi^{j+1}(t,x)+\mathfrak{m}\,\frac{e^{\phi^j}(t,x)}{\displaystyle\int_{\mathbb{T}_x}e^{\phi^j}(t,y)\,\mathrm{d}y}=n_i(t,x),\qquad\forall j\geqslant 0.$$

This strategy does however not converge, neither with a Fourier nor with a finite difference discretization, and this due to stability reasons brought in by the exponential term.

Instead, our numerical scheme is based on the following semi-implicit procedure

$$-\partial_{xx}\phi^{j+1}(t,x)+\mathfrak{m}\,\frac{e^{\phi^{j+1}}(t,x)}{\displaystyle\int_{\mathbb{T}_x}e^{\phi^j}(t,y)\,\mathrm{d}y}=n_i(t,x),\quad\forall j\geqslant 0,\tag{51}$$

with a further manipulation to linearize the implicit exponential term. Supposing ϕ^j known, one can write $e^{\phi^{j+1}}=e^{\phi^j}\,e^{\phi^{j+1}-\phi^j}$. Assuming furthermore that two subsequent iterations are sufficiently close, namely assuming that $\|\phi^{j+1}-\phi^j\|_{L^2(\mathbb{T}_x)}\ll 1$, one can approximate

$$e^{\phi^{j+1}-\phi^j}\simeq 1+\phi^{j+1}-\phi^j,$$

thus leading to the numerical scheme

$$-\partial_{xx}\phi^{j+1}+n^j\phi^{j+1}=n_i-n^j(1-\phi^j),\qquad\text{where}\qquad n^j=\mathfrak{m}\,\frac{e^{\phi^j}}{\displaystyle\int_{\mathbb{T}_x}e^{\phi^j(t,y)}\,\mathrm{d}y}.\tag{52}$$

This last equation can now be solved with either a finite difference scheme or a Fourier spectral method and gives good results as shown in the following.

To illustrate the convergence of our method (52), let us take the following test case : on a periodic domain $[0, L]$ of length $L = 12$, choose the ion density

$$n_i(x) = k^2 \sin(kx) + \frac{e^{\sin(kx)}}{\int_{\mathbb{T}_x} e^{\sin(ky)}\,\mathrm{d}y}, \qquad k = 2\pi/L, \quad \forall x \in [0, L].$$

In this case, the exact solution to the associated nonlinear elliptic problem (4) is $\phi^*(x) := \sin(kx)$, and hence $n^*(x) = \frac{e^{\sin(kx)}}{\int_{\mathbb{T}_x} e^{\sin(ky)}\,\mathrm{d}y}$.

We choose for this test case a standard second order finite difference discretization of (52) with several grids Δx, and an initial guess $\phi^{j=0} = 0$. In Figure 1, the error on the spatial densities $\|n^j - n^*\|_{L^2(\mathbb{T}_x)}$ (left) and the error on the electric potential (right) are both plotted with respect to the iteration number j. Since the constraint on the asymptotic electric potential $\int_{\mathbb{T}_x} \phi^*\,\mathrm{d}x = 0$ is not necessarily compatible with the various iterations ϕ^j, we plot the L^2-error between the iterated electric potential with rescaled average $\phi^j - \frac{1}{|\mathbb{T}_x|}\int_{\mathbb{T}_x} \phi^j\,\mathrm{d}x$ and the asymptotic electric potential ϕ^*. What can be remarked is that after very few iterations ($j = 3$), the iterative procedure gives an acceptable result, the order of magnitude being negligible when compared to the amplitude of the limit problem solution. Numerically the convergence rate is of order 2 in Δx.

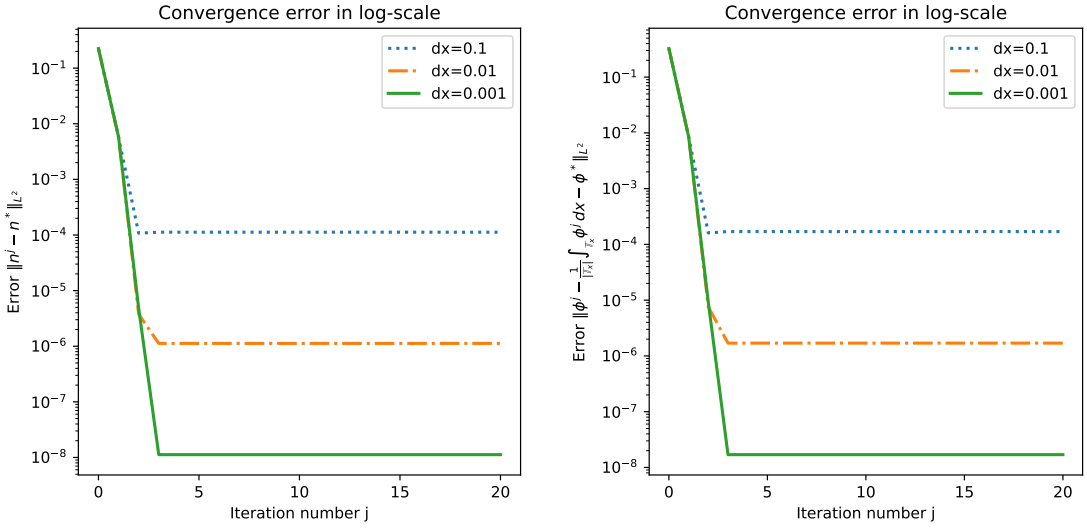

FIGURE 1. Left: Convergence of the density $n^j = \mathfrak{m}\frac{e^{\phi^j}}{\int_{\mathbb{T}_x} e^{\phi^j(y)}\,\mathrm{d}y}$ computed via (52) towards the exact density n^* of the limit problem (4). Right: Convergence of ϕ^j - after rescaling its average to 0 - towards the exact electric potential ϕ^*

6.2. **Numerical Scheme for the Kinetic problem with not too small $\varepsilon > 0$.** We shall now present a numerical scheme for the resolution of the Vlasov-Poisson-Fokker-Planck system

$$\begin{cases} \partial_t f^\varepsilon + \dfrac{1}{\varepsilon} v\,\partial_x f^\varepsilon - \dfrac{1}{\varepsilon} E^\varepsilon\,\partial_v f^\varepsilon = \dfrac{1}{\varepsilon}\partial_v\left[v\,f^\varepsilon + \partial_v f^\varepsilon\right], \\ -\partial_{xx}\phi^\varepsilon = n_i - n^\varepsilon, \qquad E^\varepsilon = -\partial_x \phi^\varepsilon\,. \end{cases}$$

In the velocity space, we shall make use of a complete, orthogonal Hermite basis to approach the distribution functions (Hermite spectral method). For the space discretization, due to the periodicity, a standard Fourier spectral method is used. In the present section, $\varepsilon \in (0, 1]$ is chosen not too small, the numerical procedure requiring a time-step Δt of order ε. In the next section, however, we will adapt this method in such a manner to recover automatically for $\varepsilon \to 0$ the limit problem, and this with an ε-independent mesh (*Asymptotic-Preserving* procedure).

6.2.1. *Discretization in the velocity variable.*

Let us start with expanding the electron distribution function $f^\varepsilon(t,x,v)$ as in (20), and truncate it at $k = N_v - 1$, where N_v is the number of considered Hermite modes. Thus the exact solution $(f^\varepsilon, E^\varepsilon)$ of (1) is approximated by the couple $(f^\varepsilon_{N_v}, E^\varepsilon_{N_v})$ defined through

$$f^\varepsilon_{N_v}(t,x,v) := \sum_{k=0}^{N_v-1} \alpha^\varepsilon_k(t,x)\,\psi_k(v)\,, \quad E^\varepsilon_{N_v} = -\partial_x\phi^\varepsilon_{N_v}, \quad -\partial_{xx}\phi^\varepsilon_{N_v} = n_i - \alpha^\varepsilon_0, \tag{53}$$

where $\{\psi_k\}_{k\in\mathbb{N}}$ are the Hermite basis-functions defined in (21). In this section the constraint $\int_{\mathbb{T}_x}\phi^\varepsilon_{N_v}\,\mathrm{d}x \equiv 0$ determines uniquely $\phi^\varepsilon_{N_v}$, for all $\varepsilon \geqslant 0$. The coefficients $\alpha^\varepsilon_k(t,x)$ are still to be determined by solving the coupled PDE-system

$$\varepsilon\,\partial_t\alpha^\varepsilon_k(t,x) + \sqrt{k}\,\partial_x\alpha^\varepsilon_{k-1} + \sqrt{k+1}\,\partial_x\,\alpha^\varepsilon_{k+1} + E^\varepsilon(t,x)\,\sqrt{k}\,\alpha^\varepsilon_{k-1} + k\alpha^\varepsilon_k = 0\,, \quad \forall k\in\{0,\dots,N_v-1\}\,, \tag{54}$$

where we set $\alpha^\varepsilon_{-1} = \alpha^\varepsilon_{N_v} = 0$. For the sake of notational simplicity, we denote from now on again $(f^\varepsilon, E^\varepsilon)$, instead of $(f^\varepsilon_{N_v}, E^\varepsilon_{N_v})$ for the truncated solution. This system is a closed system, coupled with Poisson's equation, and is well posed in $(L^2([0,T]\times\mathbb{T}_x))^{N_v}\times L^\infty([0,T]\times\mathbb{T}_x)$. Letting formally ε tend towards zero in (54) yields the PDE-hierarchy

$$\begin{cases} \sqrt{k}\,\partial_x\alpha^0_{k-1} + \sqrt{k+1}\,\partial_x\,\alpha^0_{k+1} + E^0(t,x)\,\sqrt{k}\,\alpha^0_{k-1} + k\alpha^0_k = 0 \\ -\partial_{xx}\phi^0 = n_i - \alpha^0_0, \qquad E^0 = -\partial_x\phi^0\,. \end{cases} \tag{55}$$

By equivalence with the Limit-model (4), one proves the well-posedness of this PDE-system, with a solution satisfying $\alpha^0_k \equiv 0$ for $k \neq 0$ and α^0_0 solution of the limit-problem

$$\begin{cases} \partial_x\alpha^0_0 - \partial_x\phi^0\,\alpha^0_0 = 0\,, \\ -\partial_{xx}\phi^0 = n_i - \alpha^0_0, \qquad E^0 = -\partial_x\phi^0\,, \end{cases} \tag{56}$$

associated with the constrint of zero average.

6.2.2. *Discretization in the space variable.*

Dealing with a periodic framework in $x \in \mathbb{T}_x$, one can treat the discretization in the space variable via a Fourier spectral method. One approximates thus the Hermite coefficients $\alpha^\varepsilon_k(t,x)$ and the potential function $\phi^\varepsilon(t,x)$ as follows

$$\alpha^\varepsilon_k(t,x) \simeq \alpha^{\varepsilon,N_x}_k(t,x) := \sum_{l=-N_x}^{N_x} \alpha^\varepsilon_{k,l}(t)\,e^{\frac{2\pi\mathbf{i}\,lx}{L}}\,, \qquad \phi^\varepsilon(t,x) \simeq \phi^\varepsilon_{N_x}(t,x) := \sum_{l=-N_x}^{N_x} \beta^\varepsilon_l(t)\,e^{\frac{2\pi\mathbf{i}\,lx}{L}}\,, \tag{57}$$

with $L := |\mathbb{T}_x|$ and $2N_x+1$ considered Fourier modes. Again, for notational simplicity, we drop the N_x exponent, keeping in mind that all of the considered numerical quantities have their Fourier decomposition truncated at order N_x.

We decompose the ion and electron density as

$$n_i(x) := \sum_{l=-N_x}^{N_x} \widehat{n_{i,l}}\,e^{\frac{2\pi\mathbf{i}\,lx}{L}}\,, \qquad n^\varepsilon(t,x) = \alpha^\varepsilon_0(t,x) := \sum_{l=-N_x}^{N_x} \alpha^\varepsilon_{0,l}(t)\,e^{\frac{2\pi\mathbf{i}\,lx}{L}}\,,$$

and plug this decomposition into (54), yielding the following coupled ODE system

$$\begin{aligned} \varepsilon\,\alpha^\varepsilon_{k,l}{}'(t) + \left(\frac{2\pi\mathbf{i}\,l}{L}\right)\sqrt{k}\,\alpha^\varepsilon_{k-1,l}(t) + \left(\frac{2\pi\mathbf{i}\,l}{L}\right)\sqrt{k+1}\,\alpha^\varepsilon_{k+1,l}(t) + k\,\alpha^\varepsilon_{k,l}(t) \\ -\sqrt{k}\sum_{\substack{m=-N_x \\ l-m\in\{-N_x,\dots,N_x\}}}^{N_x} \left(\frac{2\pi\mathbf{i}\,(l-m)}{L}\right)\beta^\varepsilon_{l-m}(t)\,\alpha^\varepsilon_{k-1,m}(t) = 0\,, \end{aligned} \tag{58}$$

for $k \in \{0, \cdots, N_v - 1\}$ and $l \in \{-N_x, \cdots, N_x\}$. The nonlinear coupling is due to Poisson's equation

$$\left(\frac{2\pi l}{L}\right)^2 \beta_l^\varepsilon(t) = \widehat{n_{i,l}} - \alpha_{0,l}^\varepsilon(t)\,, \quad \forall l \in \{-N_x, \cdots, N_x\}\,,$$

and we impose $\beta_l^\varepsilon = 0$ if $l \notin \{-N_x, \cdots, N_x\}$, and also for $l = 0$ due to the potential constraint of zero mean. .

Thus, using a Hermite method in the variable v and a Fourier method in the variable x leads to a system of ODE equations for the computation of the Hermite-Fourier coefficients $\alpha_{k,l}^\varepsilon(t)$. Coupling between the different modes arises from particle streaming as well as from the non-linear term involving the electric potential. To simplify the notation, let us introduce the vector $W^\varepsilon(t) := \{\alpha_{k,l}^\varepsilon(t)\}_{k,l}$ and rewrite this ODE system (58) simply as

$$\varepsilon \frac{\mathrm{d}}{\mathrm{d}t} W^\varepsilon(t) + B(t)\, W^\varepsilon(t) = 0\,, \quad \forall t \in [0, T]\,, \tag{59}$$

where we underline that the matrix $B(t)$ depends on W.

Remark 8. *Usually, when dealing with spectral methods, and notably for the Vlasov-Poisson equation, Gibbs effects appear due to filamentation. Due to particle streaming, there is a coupling between various Hermite modes, propagating perturbations towards low order modes. This effect is called recurrence. To solve these problems, a filter is usually applied on high-order modes. Thankfully, as opposed to Vlasov-Poisson system, in the Vlasov-Poisson-Fokker-Planck case the collision operator has a strong smoothing effect, and strongly dissipates high order modes. The mixing properties of the transport operator permits to propagate this gain of regularity in the space variable, and therefore filamentation does not occur. Because of these facts, it is not necessary to apply a filter in order to damp artificially high-order Hermite-Fourier coefficients.*

6.2.3. *Discretization in time.*

The last step concerns the time-discretization of the ODE system (59). In the following, we will omit the exponent ε, and we dedicate the exponent index to the iteration in time.

Let us discretize homogeneously the time interval $[0, T]$ into N_t sub-intervals via $t^j := j\,\Delta t$ where $j = 0, \ldots, N_t$, and $\Delta t := T/N_t$, and approximate (59) via the Euler implicit scheme

$$\varepsilon \frac{W^{j+1} - W^j}{\Delta t} + B^{j+1} W^{j+1} = 0\,, \tag{60}$$

where B^j is given through $\beta_l^j \simeq \beta_l(t^j)$, computed with the help of Poisson's equation, in other words

$$\left(\frac{2\pi l}{L}\right)^2 \beta_l^j = \widehat{n_{i,l}(t_j)} - \alpha_{0,l}^j\,, \quad \forall l \in \{-N_x, \cdots, N_x\}\backslash\{0\}\,, \quad \beta_0^j := 0. \tag{61}$$

Thus we observe that for every time iteration of (60) we have to solve a nonlinear equation and for its resolution we use a fixed point technique. Fix $j \in \{0, \ldots, N_t\}$ and start the fixed point procedure by setting $W^{j,0} := W^j$. Then we construct an iterative sequence $\{W^{j,m}\}_{m\in\mathbb{N}}$ via

$$\varepsilon \frac{W^{j,m+1} - W^j}{\Delta t} + B^{j,m} W^{j,m+1} = 0\,, \quad \forall m \in \mathbb{N}.$$

We observe numerically that the sequences $\{W^{j,m}\}_{m\in\mathbb{N}}$, $\{B^{j,m}\}_{m\in\mathbb{N}}$ converge, as $m \to \infty$, towards the unique fixed point (W^{j+1}, B^{j+1}) solution of (60). In practice only a few $k^* = 3$ iterations are necessary to reach a close enough approximation of the requested fixed point, and we therefore set $B^{j+1} := B^{j,k^*}$ as well as $W^{j+1} := W^{j,k^*}$. The fully discretized system (60) ensures the conservation of mass, like its continuous counterpart (1), as shown in the next Proposition.

Proposition 8 (Mass conservation). *For any $N_x, N_v, N_t > 1$, $\varepsilon > 0$, consider the solution $\{(W^j, \beta^j)\}\}_{0\leqslant j\leqslant N_t}$ of the approximate system (60). Then the mass is preserved, namely, if we*

denote as before $W^j = \{\alpha^j_{k,l}\}_{\substack{0\leqslant k\leqslant N_v,\\ -N_x\leqslant l\leqslant N_x}}$, *we have the following* ***conservation of mass*** *property*

$$\alpha^j_{0,0} = \alpha^{in}_{0,0}, \quad \forall j \in \{0, \dots, N_t\}.$$

Proof. Denote the vector $e_{0,0} := {}^t[e_0, 0_{2N_x+1}, \cdots 0_{2N_x+1}]$, where $e_0 := {}^t[0, \cdots, 0, 1, 0, \cdots, 0]$ is a vector whose $(N_x+1)^{th}$ coordinate is 1. In other terms, the vector $e_{0,0}$ is the vector of the canonical basis associated to the average in space and velocity in our Hermite-Fourier framework.

The property is then a simple consequence of the fact that $e_{0,0}$ is in the kernel of B^j, for all $j \in \mathbb{N}$ by construction : the $(N_x+1)^{th}$ column of B^j is zero. □

6.3. **Numerical investigations and validation of the numerical scheme.** We shall now perform some numerical simulations based on the scheme (60)-(61) detailed above, in order to approximate the particle distribution function of (1). In the first test case, we will study the case of a time independent ion density, and the second test case will focus on the specificities due to a time-dependent ion density. The numerical procedure (60)-(61) will be validated thanks to the mathematical analysis performed in the first part of this paper, and more specifically thanks to the convergence results of Theorem 2.

6.3.1. *Test case 1 : time-independent ion density.*

In this subsection, we choose to take the following space homogeneous two-stream initial condition for the electron distribution function

$$f_0(x,v) := \frac{1}{7\sqrt{2\pi}}\left(2+5v^2\right)e^{-v^2/2} = \psi_0(v) + \frac{5\sqrt{2}}{7}\psi_2(v), \quad \forall (x,v) \in [0,L]\times\mathbb{R}_v\,, \tag{62}$$

and fix the following background ion density

$$n_i(x) = 1 + \kappa\left[\frac{\cos(2kx)+\cos(3kx)}{1.2} + \cos(kx)\right], \quad \forall x \in [0,L], \tag{63}$$

where $k = 2\pi/L$, $L = 12$, and $\kappa = 0,4$. Recall that in this context, the limit $\varepsilon \to 0$ is equivalent to the long-time asymptotics $t \to \infty$.

We plot in Figure 2 some snapshots in the (x,v) phase-space of the particle density function f^ε at several instants and for a fixed $\varepsilon = 0.01$. As one can see, the particle density function approaches very rapidly a distribution close to a Maxwellian ($t = 0.005$) in the velocity space. It is only afterwards that the mass starts to be distributed by the transport operator also in the x direction. In the long-time limit, the distribution function approaches finally the Maxwell-Boltzmann equilibrium, as will be also shown in the following plots. Remark here that due to the collision term, the plots in Figure 2 are smoothed out and the filamentation usually observed in such kind of simulations is here not observable.

In Figure 3 we displayed the time evolution of the spatial density n^ε and of the electric potential ϕ^ε. Observe that these quantities converge, as $t \to \infty$, towards the solution of the limit problem (4) computed thanks to Newton's procedure (52) and plotted also on the Figure.

Next we performed several simulations for different values of $\varepsilon \in \{0.1, 0.005\}$, and plotted in Figure 4 the evolution over time of the macroscopic error $\|n^\varepsilon\mathcal{M} - n^0\mathcal{M}\|^2_{L^2_\sigma}$, the microscopic error $\|f^\varepsilon - n^\varepsilon\mathcal{M}\|^2_{L^2_\sigma}$ and the total error $\|f^\varepsilon - n^0\mathcal{M}\|^2_{L^2_\sigma}$. The asymptotic density n^0 is computed thanks to our Newton procedure (52) discretized with a finite difference method. Notice that in Figure 4b the macroscopic error decreases quickly before saturating at a value of approximately 10^{-10}. The saturation occurs at the order of magnitude of the error obtained by the limit problem procedure (52) (see Figure 1 for this saturation). This numerical convergence matches that of Theorem 2 and therefore supports the validity of our numerical scheme (60)-(61). Notice also that letting ε become smaller is, in this situation, nothing else than accelerating the time, such that Figure 4a is a zoom of Figure 4b, showing more details in the initial layer. This Figure 4a permits to illustrate the effects of the struggle between the transport operator and the collision operator during the

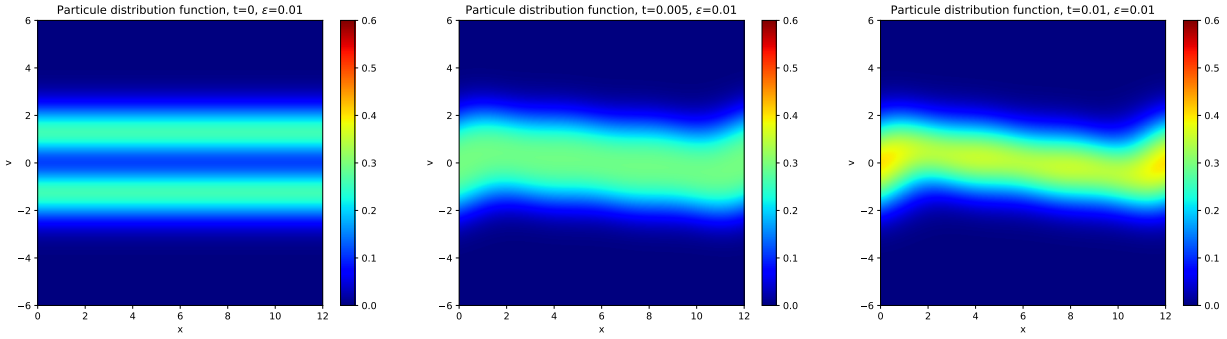

(A) t=0 (B) t=0,005 (C) t=0,01

(D) t=0,02 (E) t=0,03 (F) t=0,05

FIGURE 2. Time-evolution of the particle distribution function f^ε solution of (1), for $\varepsilon = 0.01$, $N_v = 60$, $N_x = 40$, $\Delta t = \varepsilon/40$.

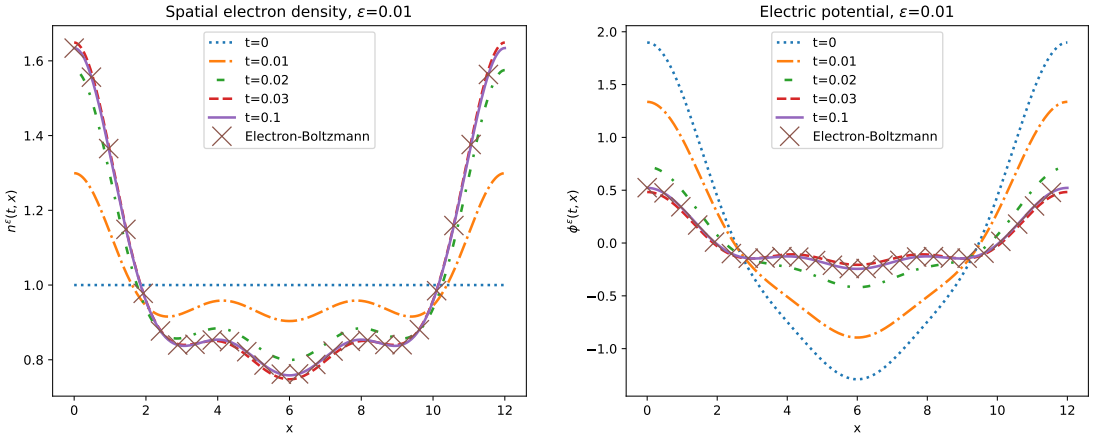

(A) n^ε (B) ϕ^ε

FIGURE 3. Snapshots at various instants of the spatial density n^ε and the electric potential ϕ^ε corresp. to the solution of (1), for $\varepsilon = 0.01$, $N_v = 60$, $N_x = 40$. The X markers correspond to the Electron-Boltzmann relation computed thanks to (52).

transient regime. The convergence towards the equilibrium arises iteratively, the collision operator reduces firstly the microscopic error at the price of a small increase of the macroscopic error, and then the transport operator becomes predominant, decreasing the macroscopic error at the price of an increased microscopic error. This is related to what is called (for instance in [33]) the interplay

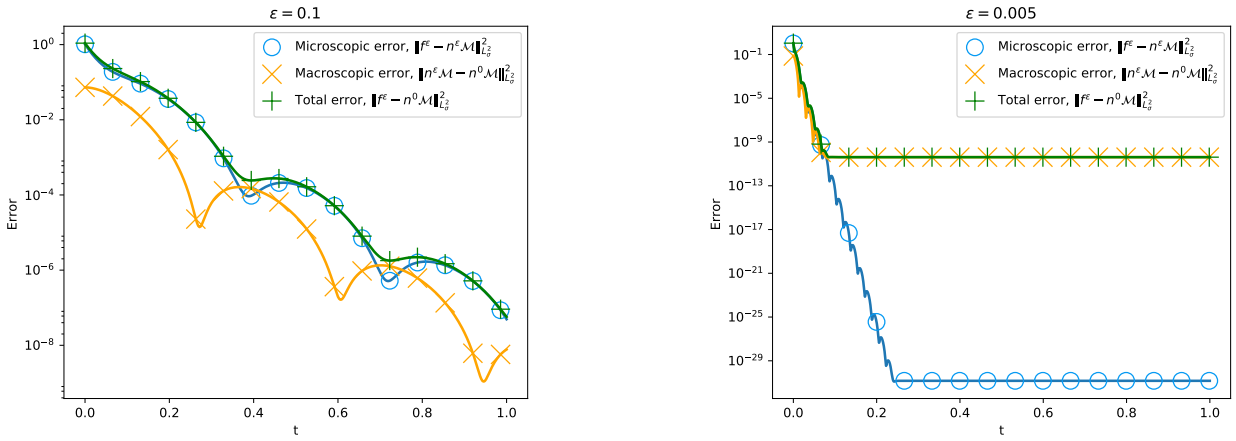

(A) ε=0.1 (B) ε=0.005

FIGURE 4. Convergence of the particle distribution function solution of (1) over time, for two different ε-values and $N_v = 20$, $N_x = 28$, $\Delta t = \varepsilon/35$.

between the dissipation introduced by the collision operator, and the conservative, mixing role played by the nonlinear, kinetic transport.

In Figure 5 we plotted the norms of several Hermite modes, thus investigating further the behaviour of the microscopic error of Figure 4 by decomposing it in several modes. One can

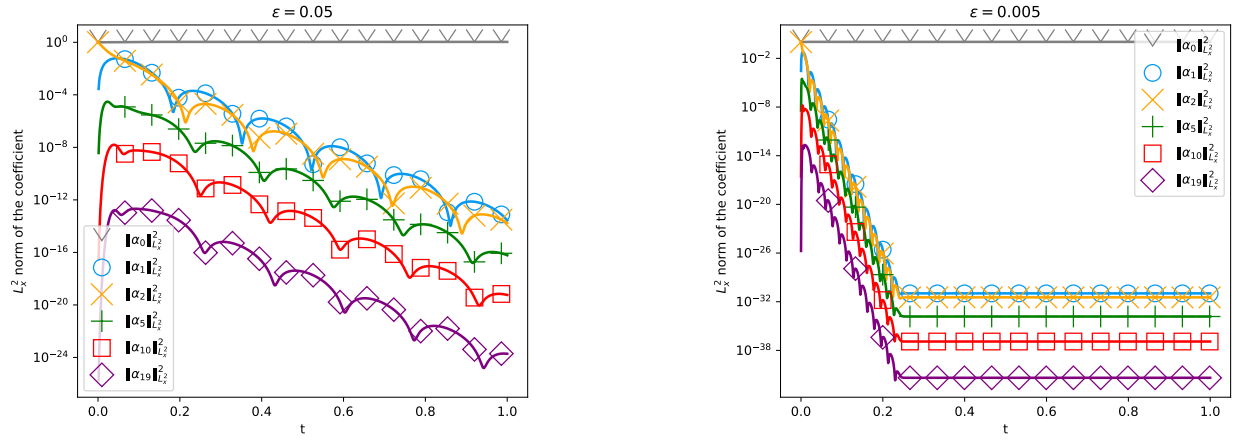

(A) ε=0.05 (B) ε=0.005

FIGURE 5. Convergence of various Hermite modes of the solution of (1) over time, $N_v = 20$, $N_x = 28$, $\Delta t = \varepsilon/35$, for various ε.

see, as expected from Theorem 2, that the norm of the first coefficient α_0 does not vanish in time. Indeed, we have seen in Figure 4 that it converges towards the solution of the limit problem. We can also notice that although the Hermite mode α_2 has a greater importance than the others at the initial time, it is quickly damped and becomes then smaller in L^2_x-norm than the coefficient α_1. Finally, due to the particle streaming induced by the transport operator, even the modes that were initially zero (namely, all of them, except α_0 and α_2), increase slightly during an initial layer before converging again towards zero.

One may wonder if this initial layer is actually of size ε in time. To investigate this, we underline that this initial layer is exactly the reason of a convergence of order $\mathcal{O}(\sqrt{\varepsilon})$ for all of the Hermite modes in (7), when considering the $L^2_{\mathrm{dt}}L^2_\sigma-$norm. To see this, one can integrate in time the result of Theorem 2, yielding, after applying the square root

$$\|f^\varepsilon - n^0\mathcal{M}\|_{L^2((0,T);L^2_\sigma(\mathbb{T}_x\times\mathbb{R}_v))} \leqslant \sqrt{\varepsilon}\,\|f^\varepsilon_{in} - n^0_{in}\mathcal{M}\|_{L^2_\sigma(\mathbb{T}_x\times\mathbb{R}_v)}\sqrt{C_0\left[1-e^{-\frac{C_1 T}{\varepsilon}}\right]} + \varepsilon\sqrt{C_2\,T},$$
$$\forall \varepsilon \leqslant \varepsilon_0, \forall t\in[0,T].$$

As one can see, the dominant term is the first one, namely, the term associated with the initial layer, and is of order $\mathcal{O}(\sqrt{\varepsilon})$ as $\varepsilon\to 0$. In this specific case of a time-independent ion density function n_i, the constant C_2 is even zero, such that we remain only with the initial layer term. The object of Figure 6, is therefore to confirm the theoretical expected rate of convergence of $\mathcal{O}(\sqrt{\varepsilon})$, which in turn confirms the size of the initial layer of our numerical scheme (60).

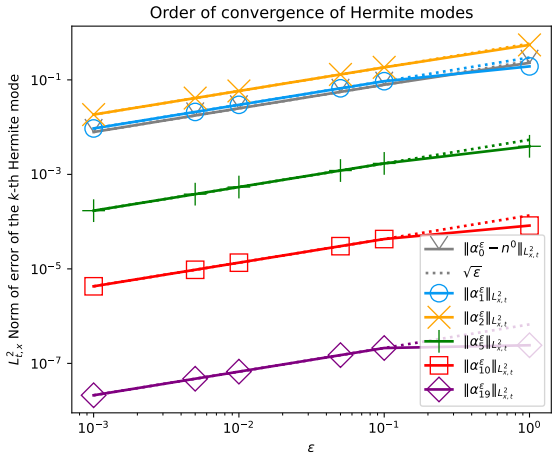

FIGURE 6. Convergence in ε of the $L^2_{t,x}$-norm of the Hermite modes of the solution of (1), for $N_v = 20$, $N_x = 28$, $\Delta t = \varepsilon/35$. The dotted lines represent a behaviour of the order of $\mathcal{O}(\sqrt{\varepsilon})$.

Corollary 1 addresses the behaviour of the Hermite coefficients with respect to their index k in the Hermite hierarchy. The object of Figure 7 is to investigate this rate of $\mathcal{O}(\sqrt{k^{-1}})$. As one can see, for small $\varepsilon \ll 1$, the convergence with respect to k is rather of order $\mathcal{O}(e^{-rk})$, with $r \simeq 0.627$. The hypocoercive study performed in this paper was in a general L^2_σ setting. Following the approach of [22] would yield a more accurate rate of convergence of order $\mathcal{O}(k^{-s/2})$, for H^s_σ initial data. Finding rigorous evidence of an exponential rate is however an open question. Finally, one can notice that the very last computed Hermite coefficient seems not to follow this exponential trend. This is a numerical artefact due to the brutal truncation of the Hermite hierarchy in (54).

6.3.2. *Test case 2 : time-dependent ion density.* In this test case, we choose the following space inhomogeneous two-stream initial condition

$$f_{in}(x,v) := \left(\frac{4}{7} + 0.4\cos(2kx) + \frac{3}{7}v^2\right)\frac{e^{-v^2/2}}{\sqrt{2\pi}} = [1+0.4\cos(2kx)]\psi_0(v) + \frac{3\sqrt{2}}{7}\psi_2(v), \tag{64}$$

and a time-dependent ion density n_i, defined as follows

$$n_i(t,x) := 1 + \kappa\sin(4\pi t)\left[\frac{\cos(2kx)+\cos(3kx)}{1.2} + \cos(kx)\right], \quad \forall x\in[0,L], \tag{65}$$

with $k = 2\pi/L$, $L = 12$, and $\kappa = 0,3$.

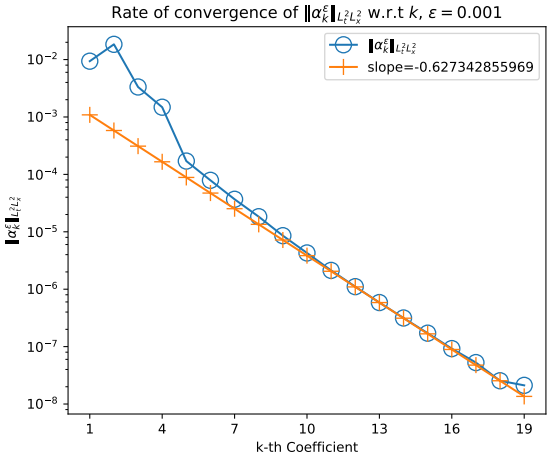

FIGURE 7. $L^2_{t,x}$-norm of the Hermite coefficients of the solution of (1), as a function of k (log-scale) and for $N_v = 20$, $N_x = 28$, $\Delta t = \varepsilon/35$, $\varepsilon = 0.001$.

This time, the result of Theorem 2 still predicts an initial layer of size ε in time, but also an error of size ε^2 during the permanent regime. This is closely related to the fact that, as underlined in Remark 7, if n_i depends on time, the constant C_2 in Theorem 2 is non-zero and depends only on $\partial_t n^0$. This effect is illustrated in Figure 8. Notice also that the error schrinks dramatically at the times at which $\partial_t n_i$ becomes zero (namely at times $t = 1/8,\ 3/8,\ 5/8,\ 7/8$).

We also plotted in Figure 9a the rate of convergence of various Hermite coefficients with respect to ε, and confirm again the rate of convergence $\mathcal{O}(\sqrt{\varepsilon})$ of (7). We see that our scheme renders accurately the order of magnitude of the initial layer even when the permanent regime is nontrivial.

One can then wonder if the size of the permanent regime is accurately computed. For this, note that our Theorem 2 predicts that

$$\sup_{t\in[s,T]} \|f^\varepsilon(t) - f^0(t)\|^2_{L^2_\sigma} = \mathcal{O}(\varepsilon^2), \qquad \text{as } \varepsilon \to 0, \quad \forall\, 0 < s < T.$$

We plotted in Figure 9b the macroscopic error $\sup_{t\in[T/2,T]} \|n^\varepsilon(t)\mathcal{M} - n^0(t)\mathcal{M}\|^2_{L^2_\sigma}$ and the microscopic one $\sup_{t\in[T/2,T]} \|n^\varepsilon(t)\mathcal{M} - n^0(t)\mathcal{M}\|^2_{L^2_\sigma}$ in the permanent regime. As one can see, they are both numerically of order $\mathcal{O}(\varepsilon^2)$, and we conclude that indeed the scheme renders accurately the permanent regime.

Finally we mention that the numerical conservation of mass is guaranteed up to machine precision for reasonably small $\varepsilon > 0$ (up to about $\varepsilon \simeq 10^{-3}$).

7. Asymptotic preserving approach

The focus of this section is the investigation of the asymptotic properties of our numerical scheme (60)-(61) when ε becomes smaller and smaller. In order to get an *Asymptotic-preserving* (AP) scheme which shall permit the choice of an ε-independent time step Δt, we shall slightly reformulate the previous scheme.

7.1. Enforcing the numerical mass conservation.

Our first problem in the $\varepsilon \to 0$ limit concerns the numerical mass conservation. The constraint $\int_{\mathbb{T}_x} n^\varepsilon(t,x)\,\mathrm{d}x \equiv \mathfrak{m}$ shall be valid for all $\varepsilon \geqslant 0$, in particular also in the limit. However one remarks that solving (60) for $\varepsilon = 0$ loses this mass conservation. Reformulated in other words, the condition number of the matrix $(\varepsilon I_{N_v(2N_x+1)} + \Delta t\, B^{j+1})$ is of order ε^{-1}.

To cope with this problem, we can multiply the $(N_x+1)^{th}$ - line of the system

$$(\varepsilon I_{N_v(2N_x+1)} + \Delta t\, B^{j+1})\, W^{j+1} = \varepsilon W^j\,,$$

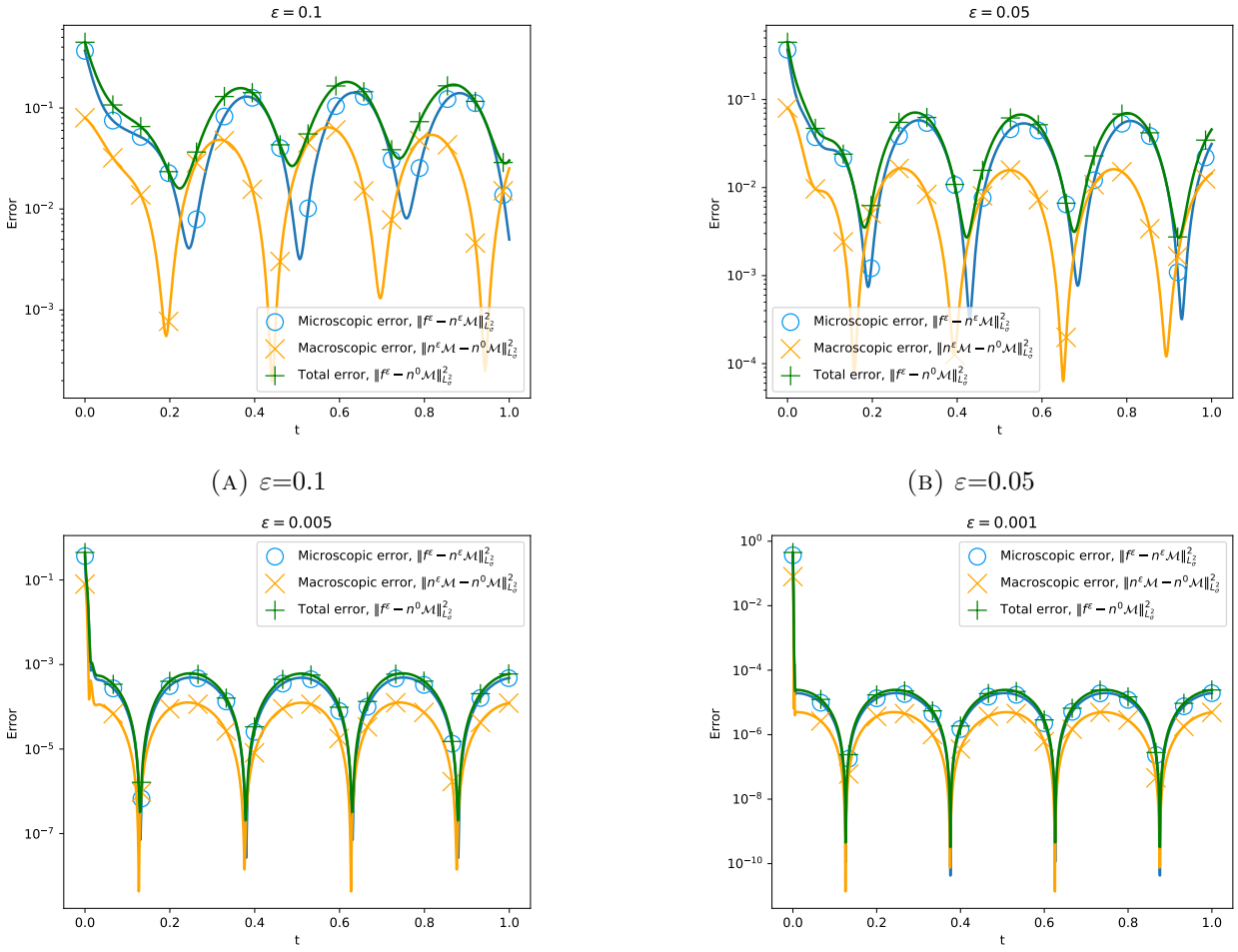

(A) ε=0.1 (B) ε=0.05

(C) ε=0.005 (D) ε=0.001

FIGURE 8. Convergence of the particle distribution function solution of (1) over time, $N_v = 20$, $N_x = 28$, $\Delta t = \varepsilon/35$, for various ε.

by ε^{-1}, line which corresponds to the mass conservation. This leads to an equivalent mathematical problem for $\varepsilon > 0$, all the while numerically guaranteeing a non singular condition number of the matrix, and being compatible with the limit $\varepsilon \to 0$. Heuristically, we enforced the numerical conservation of mass, for all $\varepsilon \geqslant 0$.

7.2. **Difficulties related to the computation of the limit problem.** Now that we reformulated our problem so that the limit $\varepsilon \to 0$ is regular, we focus on the accuracy of our scheme when ε becomes zero. For the sake of the exposition, we shall omit here to underline again the multiplication by ε^{-1} of the $(N_x+1)^{th}$ line of system (60), but we shall keep in mind that the conservation of the mass must be ensured for the matrices to be invertible in the limit $\varepsilon \to 0$.

We plotted in Figure 10 the evolution over time of the microscopic and macroscopic errors for the solution of (1) thanks to procedure (60)-(61), with the additional enforcing of the mass conservation, but this time, we took $\Delta t > \varepsilon$. Compare now both Figures 10 and 8d, the only different parameter being the time-step. As one can see, in Figure 10, the microscopic part of the particle distribution function gets immediately damped, as expected, but the macroscopic part fails to converge towards the desired limit problem. The convergence problem therefore lies at the macroscopic level. To investigate this problem, we examine our numerical procedure when ε becomes smaller.

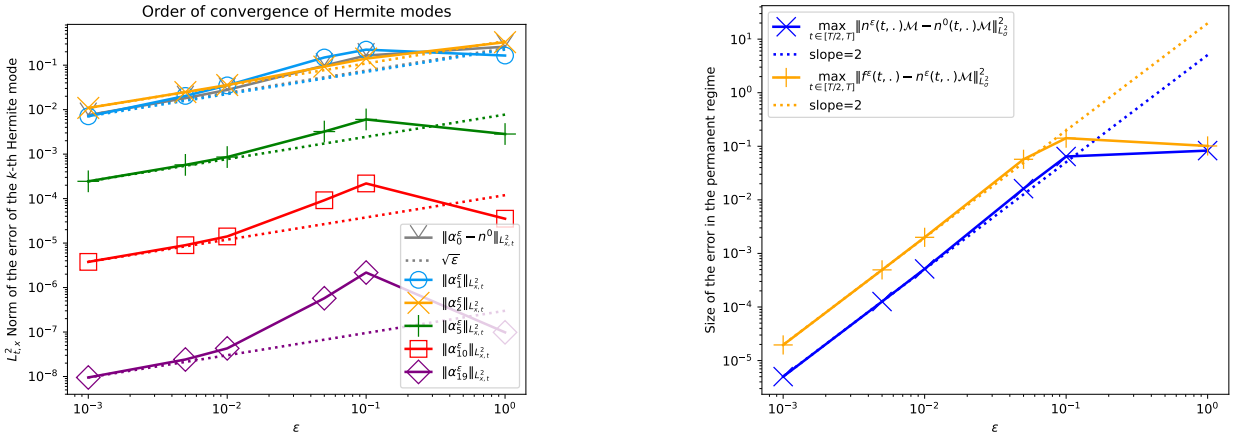

(A) (B)

FIGURE 9. $N_v = 20$, $N_x = 28$, $\Delta t = \varepsilon/35$ (A) $L^2_{t,x}-$convergence of various Hermite modes, the dotted lines represent a behaviour of $\mathcal{O}(\sqrt{\varepsilon})$. (B) Size of the (squared) error in the permanent regime, the dotted lines represent a behaviour of $\mathcal{O}(\varepsilon^2)$.

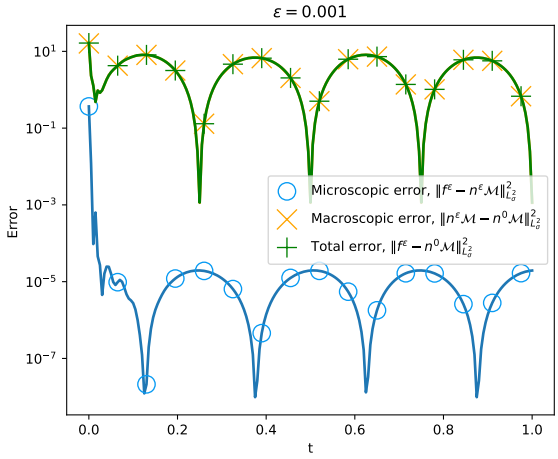

FIGURE 10. Default of convergence of the particle distribution function solution of (1) (method (60)) for $\Delta t = 0.005 > \varepsilon = 0.001$ and $N_v = 20$, $N_x = 28$, $\Delta t = 0.005$

The procedure obtained when taking $\varepsilon = 0$ in (60)-(61) is a naive fixed point technique for the resolution of

$$B^{j+1} W^{j+1} = 0. \tag{66}$$

Sadly, this procedure does not converge, and for this reason, neither does our numerical scheme (60)-(61) when $\varepsilon < \Delta t$. Actually, the same difficulty arises when trying to solve the limit problem (which is macroscopic) not by a Newton procedure, as we did in (52), but with a naive fixed point of the form

$$\begin{cases} \partial_x n^j - \partial_x \phi^j n^j = 0, \\ -\partial_{xx} \phi^{j+1} = n_i - n^j, \end{cases}$$

with either a Fourier or a finite difference discretization (see Section 6.1).

In order to cope with this difficulty, rather than computing directly a numerical approximation of the full distribution function f^ε, we are going to use the decomposition introduced in the proof of Theorem 2, namely in the asymptotic and the fluctuation part.

7.3. **Separate computation of the fluctuation and the limit part.** Thanks to the procedure (52), we have access to the limit particle density function f^0 given by the resolution of the limit problem (4). Now, rather than directly computing the particle distribution function f^ε, we decide to decompose $f^\varepsilon = f^0 + g^\varepsilon$ and to expand the fluctuating part in the Hermite basis as

$$g^\varepsilon(t,x,v) = \sum_{k=0}^{N_v-1} \gamma_k^\varepsilon(t,x)\,\psi_k(v),$$

with the coefficients $\{\gamma_k\}_k$ satisfying the following truncated PDE-system

$$\begin{cases} \varepsilon\,\partial_t\gamma_0^\varepsilon + \partial_x\gamma_1^\varepsilon = -\varepsilon\partial_t n^0, \\ \varepsilon\,\partial_t\gamma_1^\varepsilon + \partial_x\gamma_0^\varepsilon - \partial_x\phi^\varepsilon\gamma_0^\varepsilon + \sqrt{2}\partial_x\gamma_2^\varepsilon - \partial_x\varphi^\varepsilon n^0 + \gamma_1^\varepsilon = 0, \\ \varepsilon\,\partial_t\gamma_k^\varepsilon + \sqrt{k}\,\partial_x\gamma_{k-1}^\varepsilon - \sqrt{k}\,\partial_x\phi^\varepsilon\gamma_{k-1}^\varepsilon + \sqrt{k+1}\,\partial_x\gamma_{k+1}^\varepsilon + k\gamma_k^\varepsilon = 0\,, \quad \forall k\in\{2,\dots,N_v-1\} \\ -\partial_{xx}\varphi^\varepsilon = -\gamma_0^\varepsilon, \qquad \phi^\varepsilon = \phi^0 + \varphi^\varepsilon, \end{cases} \tag{67}$$

with $\gamma_{-1} = \gamma_{N_v} \equiv 0$. As we did before, we discretize this equation (67) with an implicit Euler-Fourier spectral approach. Thus our AP-strategy is based on the resolution of (52) for the macroscopic part and (67) for the microscopic part.

7.4. **Analysis of the AP-Scheme.** Let us now study the AP properties of the scheme based on the fluctuation computation. An AP-scheme should be stable and uniformly accurate with respect to the small parameter ε, for a fixed mesh.

To illustrate that this is the case, we first start by fixing a time step $\Delta t = 0.005$. In Figure 11, we computed the spatial density of electrons n^ε and the electric potential ϕ^ε for various values of ε. We

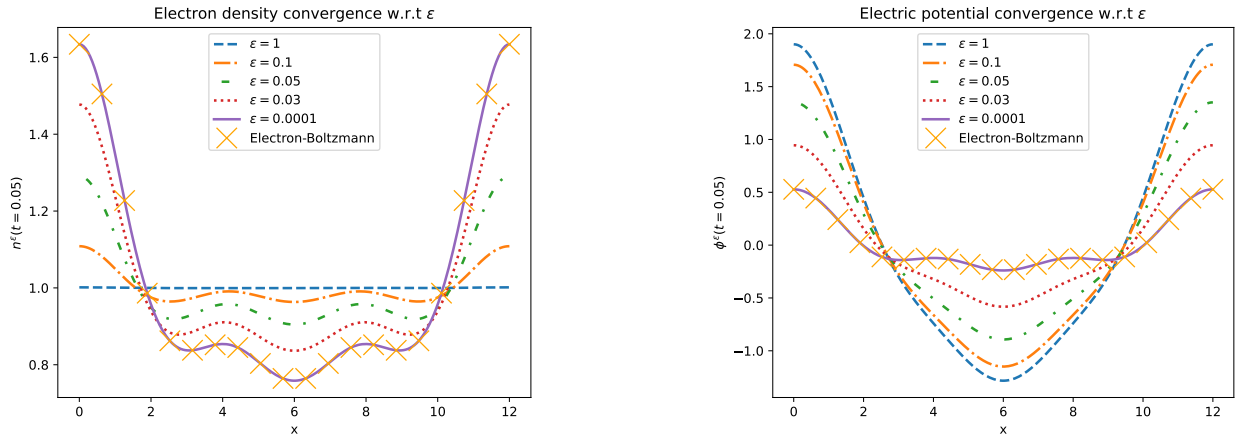

(A) $n^\varepsilon(t=0.05)$ (B) $\phi^\varepsilon(t=0.05)$

FIGURE 11. Spatial density n^ε and electric potential ϕ^ε computed with our AP-method for various ε and fixed $t = 0.05$, with $N_v = 20$, $N_x = 20$, $\Delta t = 0.005$. The ion density n_i is chosen as in (63).

chose in this case to take the time-independent ion spatial density n_i as in (63), and the associated initial condition (62). In this case the $\varepsilon \to 0$ limit is equivalent to the $t \to \infty$ limit, which explains the resemblance between Figures 11 and 3. In Figure 11, the scheme has the correct behaviour even when $\varepsilon \ll \Delta t$.

Let us now investigate the accuracy of our numerical scheme. For this, we take the spatial ion density n_i to be time-dependent, as given by (65), and the associated initial condition (64). Firstly, we test our numerical scheme on its ability to successfully pass the initial layer. As we reminded before, the solution f^ε of (1) should verify the following uniform estimate in the permanent regime

$$\sup_{t\in[\Delta t,T]} \|f^\varepsilon(t) - f^0(t)\|^2_{L^2_\sigma} = \mathcal{O}(\varepsilon^2), \quad \text{as } \varepsilon \to 0, \quad \forall \Delta t > 0.$$

Our Figure 12 validates this rate of uniform in time convergence. This shows that our numerical scheme successfully passes the initial layer after a single iteration Δt, even for very small $\varepsilon \ll \Delta t$.

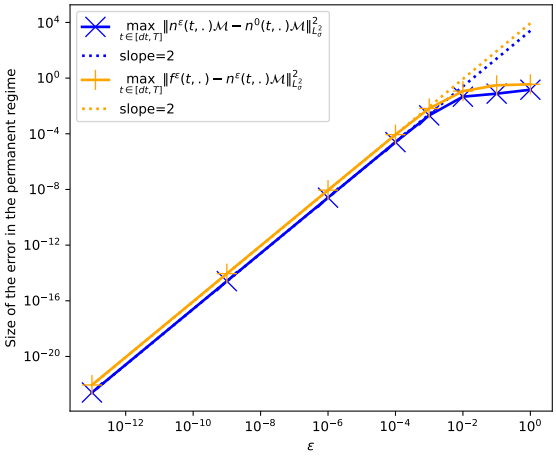

FIGURE 12. ε-Behaviour of the microscopic/macroscopic errors of the AP-method right after the first time step, with $\Delta t = 0.005$, $N_v = 20$, $N_x = 20$. The ion density n_i is chosen as in (65), $\kappa = 0.3$. The dotted lines represent a behaviour of $\mathcal{O}(\varepsilon^2)$.

We then examine how the accuracy of our AP procedure is affected by the time-step, both during the initial layer, and during the permanent regime. In Figure 13, we plotted the macroscopic error

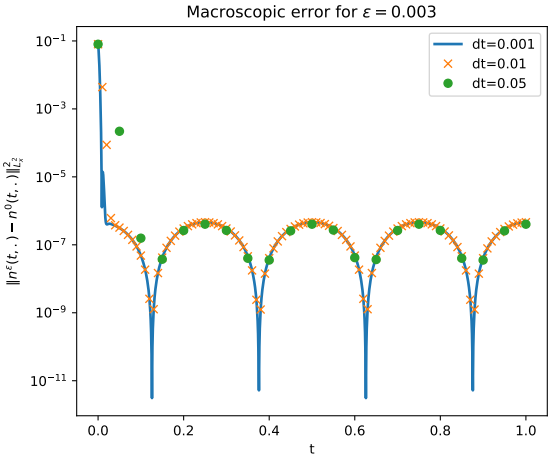

FIGURE 13. Behaviour of the macroscopic error of (1) (AP-method) during the initial layer and in the permanent regime for various time-steps Δt. $N_v = 20$, $N_x = 20$, $\varepsilon = 0.003$. The ion density n_i is chosen as in (65), $\kappa = 0.03$.

over time, with various time-steps Δt and fixed $\varepsilon = 0.003$. First, let us compare the case of $\Delta t = 0.01$

ε	Classical method (60), $\Delta t = \varepsilon/35$	AP method, $\Delta t = 0.01$	AP method, $\Delta t = 0.001$
1	20.51	63.44	682.94
0.1	208.84	63.41	613.14
0.05	418.54	64.65	616.57
0.01	2089.01	67.41	619.32
0.005	4190.13	67.40	646.47
0.001	22050.36	67.23	618.41
Limit problem	None	36.34	330.88

TABLE 1. Computation time of the different methods, in seconds, for various time steps and values of ε. $N_x = 28$, $N_v = 20$. The ion spatial density is taken time-dependent as in (65), $\kappa = 0.3$.

and $\Delta t = 0.001$. As one can see, in both cases, the permanent regime is accurately represented. The only difference lies in the treatment of the initial layer : for the case of $\Delta t = 0.001$, since the time step is small when compared to ε, the initial layer is represented with precision. When $\Delta t = 0.01$, the time step is of the same order of magnitude as ε, and thus the details of the initial layer are not rendered accurately, but without impairing the precision of the permanent regime, and with a lower computational cost. When taking an even bigger time step $\Delta t = 0.05$, the details of the initial layer are completely forgotten, but the macroscopic error is still correctly computed.

At this point, we want to emphasize that the computational benefits of our AP-procedure are important for small values of ε, because of the ε-independence of the time-step. We gathered in Table 1 the computational times of the classical method (60), which does not converge for $\Delta t > \varepsilon$, and the computational times of our AP-method, for fixed time steps. Remark that our AP-method requires to compute firsthand - and very accurately - the initial problem. Nonetheless, our method enables a robust computation, completely independently of ε, which permits to get in the end substantial computational gains (see also last line of the Table).

Finally, our AP-method enables also a substantial gain in memory: for $\varepsilon = 0.001$, the classical method with $\Delta t = \varepsilon/35$ produced a 1.7GB file containing the state of the system at all times. For the AP-method, this time with $\Delta t = 0.001$, the file weighted only 49.1MB. In both cases we took $N_x = 28$, $N_v = 20$.

Concluding, the AP-scheme is very useful if one is interested in solving the singular kinetic problem in the small $\varepsilon \ll 1$ regime, but without being interested in all details, meaning when one wants to choose a large time-step $\Delta t \gg \varepsilon$, thus being rather interested in the macroscopic behaviour of the system.

8. CONCLUDING REMARKS AND PERSPECTIVES

We shall now summarize what has been achieved in this paper, and state some of the open problems one can investigate in future works.

The aim of this article was to investigate, both from a mathematical and from a numerical point of view, the small electron-to-ion mass ratio limit $\varepsilon \to 0$ of the Vlasov-Poisson-Fokker-Planck system (1), in a setting of a given, time-dependent ion density, limit which does not correspond to the long-time asymptotics $t \to \infty$.

After a short introduction of the properties of the model (1) and a formal study of the limit $\varepsilon \to 0$, the rigorous asymptotic analysis was performed thanks to a study of the regularity of the limit problem and an adaptation of existing hypocoercivity methods to the setting of time-dependent coefficients. This analysis was performed under a condition of smallness of the initial fluctuations

(assumption (5)). This is due to our approach, which was perturbative in nature, and one may try, in future works, to lift this assumption.

Furthermore, all these studies were performed in a simplified, non-physical, one species model. In future works, one may consider similar questions regarding more physical kinetic, multispecies models with several conservation laws, such as the one developed in [14].

The numerical part of this paper was concerned with the development of a performant numerical scheme for the resolution of (1), with particular focus on the adiabatic regime $\varepsilon \to 0$. For this, a Hermite spectral approach was chosen for the discretization in the velocity variable. This choice is relevant for this asymptotic regime, as the Hermite coefficients vanish in the limit $\varepsilon \to 0$ (except the principal mode), the rate of convergence being dependent on their position in the hierarchy (see Corollary 1). This permits in practice to consider only few Hermite modes for $\varepsilon \ll 1$, and reduces thus dramatically the computational costs.

The numerical computations have however to be treated with care, especially for the time-discretization of this problem, due to the fact that the problem is stiff in time. Thanks to a reformulation and an implicit time-discretization, we were able to treat this problem as a regular limit, which led to the obtention of an *Asymptotic-Preserving* (AP) reformulation. The latter permits to choose an ε-independent time step, saving furthermore computational time.

The numerical analysis of the here presented AP-scheme as well as the construction of an AP-scheme for the more physical two-species model developed in [14] will be the object of future works.

9. Appendix

This Appendix regroups some lemmata and proofs useful for the paper, regrouped here to render the reading of the paper simpler.

9.1. Uniform in time Poincaré inequality.

In this subsection, we mention the following elementary uniform in time Poincaré inequality, in the setting of a time-dependent weight. This inequality is essential for estimates such as the macroscopic coercivity (35) or inequality (41).

Lemma 5 (Uniform in time Weighted Poincaré Inequality)**.** *Let $\phi^0 \in L^\infty((0,T)\times\mathbb{T}_x)$ such that $\int_{\mathbb{T}_x} e^{\phi^0(t,x)}\,\mathrm{d}x \equiv 1$. Then, denoting the weighted average by $\langle u\rangle_t := \int_{\mathbb{T}_x} u(x)e^{\phi^0(t,x)}\,\mathrm{d}x$, we state the following uniform in time Poincaré inequality : there exists a time-independent constant $C_P > 0$ such that*

$$C_P \int_{\mathbb{T}_x} |u(x) - \langle u\rangle_t|^2 e^{\phi^0(t,x)}\,\mathrm{d}x \leqslant \int_{\mathbb{T}_x} |\partial_x u(x)|^2 e^{\phi^0(t,x)}\,\mathrm{d}x, \qquad \forall t\in[0,T], \forall u \in H^1(\mathbb{T}_x).$$

Proof. Since the weights are very well controlled, because of the L^∞ bound of ϕ^0, we essentially present here a rough proof in one dimension of the Euclidian Poincaré-Wirtinger inequality.

Set $u \in \mathcal{C}^1(\mathbb{T}_x)$ and $y \in \mathbb{T}_x$. We compute, using Taylor's expansion

$$\begin{aligned}
|u(y) - \langle u\rangle_t| &= \left| \int_{\mathbb{T}_x} (u(y) - u(z)) e^{\phi^0(t,z)}\,\mathrm{d}z \right| \\
&\leqslant \left| \int_{\mathbb{T}_x} \int_0^1 (y-z)\partial_x u(y + s(z-y)) e^{\phi^0(t,z)}\,\mathrm{d}s\,\mathrm{d}z \right| \\
&\leqslant |\mathbb{T}_x| e^{\|\phi^0\|_\infty} \int_{\mathbb{T}_x}\int_0^1 |\partial_x u(y+s(z-y))|\,\mathrm{d}s\,\mathrm{d}z.
\end{aligned}$$

The result follows from rough estimates of the right-hand side, after squaring and integrating in $\mathrm{d}y$ against $e^{\phi^0(t,y)}$. □

9.2. **Specificities of the time-dependent case $n_i(t,x)$.** Because of the time dependency of the asymptotic electric field ϕ^0, there are some additional terms appearing in the computations, as opposed to [1]. In this subsection, we assume that α is time-dependent, and prove each point of the following lemma. This Lemma is a more detailed version of Lemma 3, giving thus the steps of the proof.

Lemma 6. *Let $\alpha \in \mathcal{C}^\infty([0,T]\times\mathbb{T}_x\times\mathbb{R}_v)$, and denote by $[A,B] := AB - BA$ the commutator. Assume that n_i satisfies the assumptions of Proposition 4, and that ϕ^0, n^0 are the electric potential and density satisfying (4), with the constraint (18). Then, if $\mathcal{T}_t$ is defined as in (25), we have the following properties:*

(1) We have the commutation relations

$$[\partial_t, (\mathcal{T}_t\Pi)^*] = 0,$$
$$\mathrm{Aux}_t\alpha := [\partial_t, (\mathcal{T}_t\Pi)]\alpha = \begin{bmatrix} 0 \\ -\partial_t\partial_x\phi^0(t,.)\cdot\alpha_0 - \partial_x\varphi_\alpha\partial_t\phi^0(t,\cdot)\cdot n^0 \\ 0 \\ \vdots \end{bmatrix}.$$

(2) One has that Aux_t is bounded uniformly with respect to time, namely

$$\|\mathrm{Aux}_t\alpha\|_t \leqslant c_*\|\alpha\|_t, \quad \forall t\in[0,T],$$

with $c_* > 0$ a time independent constant which depends on the L^∞-norm of $\partial_t\partial_x\phi^0$, $\partial_t\phi^0$ and n^0.

(3) Because of the commutation $[\partial_t, (\mathcal{T}_t\Pi)^*] = 0$, we get

$$[\partial_t, (\mathbb{I}d + (\mathcal{T}_t\Pi)^*(\mathcal{T}_t\Pi))] = (\mathcal{T}_t\Pi)^*\mathrm{Aux}_t. \tag{68}$$

(4) As a consequence we obtain

$$[\partial_t, A_t] = -A_t\mathrm{Aux}_tA_t. \tag{69}$$

This last equality (69) gives rise to the following sequence of inequalities

$$\|[\partial_t, A_t]\alpha\|_t = \|A_t\mathrm{Aux}_tA_t\alpha\|_t \leqslant \frac{1}{2}\|\mathrm{Aux}_tA_t\alpha\|_t \leqslant \frac{c_*}{2}\|A_t\alpha\|_t \leqslant \frac{c_*}{4}\|(\mathbb{I}d-\Pi)\alpha\|_t, \tag{70}$$

which is valid by density for all $\alpha \in L^\infty((0,T); l^2_0(\mathbb{N}, L^2(\mathbb{T}_x)))$. We denote $C_* := c_*/4$.

Proof. (1) First of all one notices that $(\mathcal{T}_t\Pi)^*\alpha = -\Pi\mathcal{T}_t\alpha = \begin{bmatrix} -\partial_x\alpha_1 \\ 0 \\ \vdots \end{bmatrix}$. This yields $[\partial_t, (\mathcal{T}_t\Pi)^*] = \partial_t(\mathcal{T}_t\Pi)^* - (\mathcal{T}_t\Pi)^*\partial_t = 0$. The second equality is a consequence of a direct computation on the definition of $\mathcal{T}_t$ in (25).

(2) This point is a direct consequence of the triangle inequality.

(3) We compute directly,

$$\begin{aligned}[\partial_t, (\mathbb{I}\mathrm{d} + (\mathcal{T}_t\Pi)^*(\mathcal{T}_t\Pi))] &= \{\partial_t(\mathbb{I}\mathrm{d} + (\mathcal{T}_t\Pi)^*(\mathcal{T}_t\Pi)) - (\mathbb{I}\mathrm{d} + (\mathcal{T}_t\Pi)^*(\mathcal{T}_t\Pi))\partial_t\} \\ &= \{(\mathcal{T}_t\Pi)^*\partial_t(\mathcal{T}_t\Pi) - (\mathcal{T}_t\Pi)^*(\mathcal{T}_t\Pi)\partial_t\} \\ &= (\mathcal{T}_t\Pi)^*[\partial_t, (\mathcal{T}_t\Pi)] \\ &= (\mathcal{T}_t\Pi)^*\mathrm{Aux}_t,\end{aligned}$$

where we used, for the second equality, the commutation $[\partial_t, (\mathcal{T}_t\Pi)^*] = 0$.

(4) The last point is a consequence of the multiplication of (68) on the left by the operator $(\mathbb{I}\mathrm{d} + (\mathcal{T}_t\Pi)^*(\mathcal{T}_t\Pi))^{-1}$, and on the right by A_t. On one hand, the left-hand side is computed

as follows

$$\begin{aligned}(\mathbb{I}\mathrm{d}+(\mathcal{T}_t\Pi)^*(\mathcal{T}_t\Pi))^{-1}&[\partial_t,(\mathbb{I}\mathrm{d}+(\mathcal{T}_t\Pi)^*(\mathcal{T}_t\Pi))]A_t\\ &=(\mathbb{I}\mathrm{d}+(\mathcal{T}_t\Pi)^*(\mathcal{T}_t\Pi))^{-1}[\partial_t,(\mathbb{I}\mathrm{d}+(\mathcal{T}_t\Pi)^*(\mathcal{T}_t\Pi))](\mathbb{I}\mathrm{d}+(\mathcal{T}_t\Pi)^*(\mathcal{T}_t\Pi))^{-1}(\mathcal{T}\Pi_t)^*\\ &=-[\partial_t,(\mathbb{I}\mathrm{d}+(\mathcal{T}_t\Pi)^*(\mathcal{T}_t\Pi))^{-1}](\mathcal{T}\Pi_t)^*,\end{aligned}$$

using the general computation $B^{-1}[A,B]B^{-1}=-[A,B^{-1}]$ with the operators $A=\partial_t$ and $B=(\mathbb{I}\mathrm{d}+(\mathcal{T}_t\Pi)^*(\mathcal{T}_t\Pi))$. Then, because of the commutation $[\partial_t,(\mathcal{T}_t\Pi)^*]=0$, we deduce

$$\begin{aligned}(\mathbb{I}\mathrm{d}+(\mathcal{T}_t\Pi)^*(\mathcal{T}_t\Pi))^{-1}[\partial_t,(\mathbb{I}\mathrm{d}+(\mathcal{T}_t\Pi)^*(\mathcal{T}_t\Pi))]A_t&=-[\partial_t,(\mathbb{I}\mathrm{d}+(\mathcal{T}_t\Pi)^*(\mathcal{T}_t\Pi))^{-1}](\mathcal{T}\Pi_t)^*\\ &=-[\partial_t,A_t].\end{aligned}$$

On the other hand, the right-hand side rewrites

$$(\mathbb{I}\mathrm{d}+(\mathcal{T}_t\Pi)^*(\mathcal{T}_t\Pi))^{-1}(\mathcal{T}_t\Pi)^*\mathrm{Aux}_tA_t=A_t\mathrm{Aux}_tA_t,$$

yielding the equality. The last chain of inequalities (70) follows then immediately from (38). □

9.3. **Handling the different terms in the hypocoercivity estimate (45).** For the sake of completeness, we will mention in this subsection how we deal with each of the nonlinear terms in (45).

9.3.1. *Good dissipative terms.*
The microscopic and macroscopic coercivity give the dissipation of the two first terms, namely

$$\langle\mathcal{L}\gamma^\varepsilon,\gamma^\varepsilon\rangle_t\leqslant\frac12\langle\mathcal{L}\gamma^\varepsilon,\gamma^\varepsilon\rangle_t-\frac12\|(\mathbb{I}\mathrm{d}-\Pi)\gamma^\varepsilon\|_t^2,\tag{71}$$

and

$$-\delta\langle A_t\mathcal{T}_t\Pi\gamma^\varepsilon,\gamma^\varepsilon\rangle_t\leqslant-\delta\frac{\lambda_M}{1+\lambda_M}\|\Pi\gamma^\varepsilon\|_t^2,\quad\text{using}\int_{\mathbb{T}_x}\gamma_0^\varepsilon(t,x)\,\mathrm{d}x=0.\tag{72}$$

9.3.2. *Signless terms arising in the classical computation.*
We have using (41) along with $\Pi A_t=A_t$

$$\begin{aligned}-\delta\langle A_t\mathcal{T}_t(\mathbb{I}\mathrm{d}-\Pi)\gamma^\varepsilon,\gamma^\varepsilon\rangle_t&\leqslant\delta\frac{\nu_1}{2}\|A_t\mathcal{T}_t(\mathbb{I}\mathrm{d}-\Pi)\gamma^\varepsilon\|_t^2+\delta\frac{1}{2\nu_1}\|\Pi\gamma^\varepsilon\|_t^2\\ &\leqslant\delta\Lambda^2\frac{\nu_1}{2}\|(\mathbb{I}\mathrm{d}-\Pi)\gamma^\varepsilon\|_t^2+\delta\frac{1}{2\nu_1}\|\Pi\gamma^\varepsilon\|_t^2\,,\end{aligned}\tag{73}$$

with an $\nu_1>0$ to be tuned later. Moreover we also have, using (37) and then (38) and (39)

$$\begin{aligned}\delta\,\langle\mathcal{T}_tA_t\gamma^\varepsilon,\gamma^\varepsilon\rangle_t&=\delta\,\left[\|A_t\gamma^\varepsilon\|_t^2+\|\mathcal{T}_tA_t\gamma^\varepsilon\|_t^2\right]\\ &\leqslant\frac{\delta}{4}\|(\mathbb{I}\mathrm{d}-\Pi)\gamma^\varepsilon\|_t^2+\delta\,\|(\mathbb{I}\mathrm{d}-\Pi)\gamma^\varepsilon\|_t^2\\ &=\frac{5\delta}{4}\|(\mathbb{I}\mathrm{d}-\Pi)\gamma^\varepsilon\|_t^2\,.\end{aligned}\tag{74}$$

Furthermore, using (40) and for $\nu_2>0$ to be tuned later

$$\begin{aligned}\delta\,\langle A_t\mathcal{L}\gamma^\varepsilon,\gamma^\varepsilon\rangle_t=\delta\,\langle A_t\mathcal{L}\gamma^\varepsilon,\Pi\gamma^\varepsilon\rangle_t&\leqslant\delta\frac{\nu_2}{2}\|A_t\mathcal{L}\gamma^\varepsilon\|_t^2+\frac{\delta}{2\nu_2}\|\Pi\gamma^\varepsilon\|_t^2\\ &\leqslant\delta\frac{\nu_2}{8}\|(\mathbb{I}\mathrm{d}-\Pi)\gamma^\varepsilon\|_t^2+\frac{\delta}{2\nu_2}\|\Pi\gamma^\varepsilon\|_t^2.\end{aligned}\tag{75}$$

Finally,

$$\delta\,\langle\mathcal{L}A_t\gamma^\varepsilon,\gamma^\varepsilon\rangle_t=0,\tag{76}$$

because of $\mathcal{L}(A_t)=\mathcal{L}(\Pi A_t)=(\mathcal{L}\Pi)A_t=0.A_t=0$.

9.3.3. *Terms associated with the source term.*
For some $\nu_3 > 0$ to be fixed later, Young's inequality permits to estimate

$$\varepsilon \langle \mathcal{S}, \gamma^\varepsilon \rangle_t = \varepsilon \langle \mathcal{S}, \Pi\gamma^\varepsilon \rangle_t \leqslant \frac{\nu_3 \varepsilon^2}{2\delta} \|\mathcal{S}\|_t^2 + \frac{\delta}{2\nu_3} \|\Pi\gamma^\varepsilon\|_t^2. \tag{77}$$

Since $\mathcal{S} = \Pi\mathcal{S}$, and $A\Pi = 0$, we have

$$\varepsilon\delta \langle A_t\mathcal{S}, \gamma^\varepsilon \rangle_t = 0. \tag{78}$$

Finally, using (38), Young's inequality leads to

$$\varepsilon\delta \langle A_t\gamma^\varepsilon, \mathcal{S} \rangle_t \leqslant \frac{\nu_4 \varepsilon^2 \delta}{2} \|\mathcal{S}\|_t^2 + \frac{\delta}{8\nu_4} \|(1-\Pi)\gamma^\varepsilon\|_t^2. \tag{79}$$

9.3.4. *Terms associated with the time dependency of norms and operator.*
Because of the time dependency of the norms and of the A_t operator, some small ε-order terms appear in our computations. We show how we control them. Cauchy-Schwarz' inequality immediately gives

$$-\frac{\varepsilon}{2} \sum_{k=0}^{\infty} \langle \partial_t\phi^0 \gamma_k^\varepsilon, \gamma_k^\varepsilon \rangle_{L^2_{\eta_t}(\mathbb{T}_x)} \leqslant \frac{\varepsilon}{2} \|\partial_t\phi^0\|_\infty \|\gamma^\varepsilon\|_t^2. \tag{80}$$

Thanks to (38), we have

$$-\varepsilon\delta \sum_{k=0}^{\infty} \langle \partial_t\phi^0 (A_t\gamma^\varepsilon)_k, \gamma_k^\varepsilon \rangle_{L^2_{\eta_t}(\mathbb{T}_x)} \leqslant \varepsilon\delta \|\partial_t\phi^0\|_\infty \|A_t\gamma^\varepsilon\|_t \|\gamma^\varepsilon\|_t \leqslant \frac{\varepsilon\delta}{2} \|\partial_t\phi^0\|_\infty \|\gamma^\varepsilon\|_t^2. \tag{81}$$

Finally, using (42) yields

$$-\varepsilon\delta \langle [\partial_t, A_t]\gamma^\varepsilon, \gamma^\varepsilon \rangle_t \leqslant \varepsilon\delta\, C_* \|\gamma^\varepsilon\|_t^2. \tag{82}$$

Acknowledgments. This work has been carried out within the framework of the EUROfusion Consortium, funded by the European Union via the Euratom Research and Training Programme (Grant Agreement No 101052200 — EUROfusion). Views and opinions expressed are however those of the author(s) only and do not necessarily reflect those of the European Union or the European Commission. Neither the European Union nor the European Commission can be held responsible for them. E. Lehman would like to acknowledge the financial support of the Ecole Normale Supérieure de Lyon.

References

[1] L. Addala, J. Dolbeault, X. Li, and M. L. Tayeb, *L^2-hypocoercivity and large time asymptotics of the linearized Vlasov-Poisson-Fokker-Planck system*, Journal of Statistical Physics, 184 (2021).
[2] D. Albritton, S. Armstrong, J. C. Mourrat, and M. Novack, *Variational methods for the kinetic fokker-planck equation*. Working paper or preprint, 2019.
[3] T. P. Armstrong, *Numerical studies of the nonlinear vlasov equation*, The Physics of Fluids, 10 (1967), pp. 1269–1280.
[4] M. Bessemoulin-Chatard and F. Filbet, *On the stability of conservative discontinuous galerkin/hermite spectral methods for the vlasov-poisson system*, Journal of Computational Physics, 451 (2022), p. 110881.
[5] F. Bouchut, *Existence and uniqueness of a global smooth solution for the vlasov-poisson-fokker-planck system in three dimensions*, Journal of Functional Analysis, 111 (1993), pp. 239–258.
[6] F. Bouchut and J. Dolbeault, *On long time asymptotics of the vlasov-fokker-planck equation and of the vlasov-poisson-fokker-planck system with coulombic and newtonian potentials*, Differential and Integral Equations, 8 (1995), pp. 487–514.
[7] G. Brigati, *Time averages for kinetic fokker-planck equations*. Working paper or preprint, 2021.
[8] D. Burnett, *The distribution of velocities in a slightly non-uniform gas*, Proceedings of the London Mathematical Society, s2-39 (1935), pp. 385–430.
[9] K. L. Cartwright, J. P. Verboncoeur, and C. K. Birdsall, *Nonlinear hybrid boltzmann-particle-in-cell acceleration algorithm*, Physics of Plasmas (1994-present), 7 (2000), pp. 3252–3264.
[10] Y. Chen and S. Parker, *A gyrokinetic ion zero electron inertia fluid electron model for turbulence simulations*, Phys. Plasmas, 8 (2001), pp. 441–446.

[11] P. Degond, *Global existence of smooth solutions for the vlasov-fokker-planck equation in* 1 *and* 2 *space dimensions*, Annales Scientifiques De L'Ecole Normale Superieure, 19 (1986), pp. 519–542.
[12] J. Dolbeault, C. Mouhot, and C. Schmeiser, *Hypocoercivity for linear kinetic equations conserving mass*, Transactions of the American Mathematical Society, (2015), pp. 3807–3828.
[13] J. Dominski, S. Brunner, S. K. Aghdam, T. Goerler, F. Jenko, and D. Told, *Identifying the role of non-adiabatic passing electrons in itg/tem microturbulence by comparing fully kinetic and hybrid electron simulations*, Journal of Physics: Conference Series, 401 (2012), p. 012006.
[14] F. Filbet and C. Negulescu, *Fokker-Planck multi-species equations in the Adiabatic asymptotics*. To appear in JCP, Feb. 2022.
[15] F. Filbet and T. Xiong, *Conservative discontinuous galerkin/hermite spectral method for the vlasov–poisson system*, Communications on Applied Mathematics and Computation, 4 (2020), pp. 34–59.
[16] X. Garbet, C. Bourdelle, G. T. Hoang, P. Maget, S. Benkadda, P. Beyer, C. Figarella, I. Voitsekovitch, O. Agullo, and N. Bian, *Global simulations of ion turbulence with magnetic shear reversal*, Physics of Plasmas, 8 (2001), pp. 2793–2803.
[17] N. Ghani and N. Masmoudi, *Diffusion limit of the vlasov-poisson-fokker-planck system*, Models Methods Appl. Sci. Math. Models Methods Appl. Sci, 8 (2000), pp. 463–479.
[18] H. Grad, *On the kinetic theory of rarefied gases*, Communications on Pure and Applied Mathematics, 2 (1949), pp. 331–407.
[19] F. C. Grant and M. R. Feix, *Fourier-hermite solutions of the vlasov equations in the linearized limit*, The Physics of Fluids, 10 (1967), pp. 696–702.
[20] F. Hérau, *Short and long time behavior of the fokker-planck equation in a confining potential and applications*, Journal of Functional Analysis, 244 (2005), pp. 95–118.
[21] ———, *Introduction to hypocoercive methods and applications for simple linear inhomogeneous kinetic models*, Lectures on the Analysis of Nonlinear Partial Differential Equations, 5 (2017), pp. 119–147.
[22] H. J. Hwang and J. Jang, *On the vlasov-poisson-fokker-planck equation near maxwellian*, Discrete & Continuous Dynamical Systems - B, 18 (2013), pp. 681–691.
[23] S. Jin, *Asymptotic-preserving schemes for multiscale physical problems*, Rivista di Matematica della Università di Parma, 3 (2012), pp. 177–216.
[24] D. T. K. Kwok, *A hybrid boltzmann electrons and pic ions model for simulating transient state of partially ionized plasma*, JCP, 227 (2008), pp. 5758–5777.
[25] C. Negulescu, *Asymptotic-preserving schemes. Modeling, simulation and mathematical analysis of magnetically confined plasmas*, Rivista di Matematica della Università di Parma, 4 (2013), pp. 265–343.
[26] ———, *Kinetic Modelling of Strongly Magnetized Tokamak Plasmas with Mass Disparate Particles. The Electron Boltzmann Relation*, Multiscale Modeling and Simulation: A SIAM Interdisciplinary Journal, 16 (2018), pp. 1732–1755.
[27] F. Nier and B. Helffer, *Hypoelliptic Estimates and Spectral Theory for Fokker-Planck Operators and Witten Laplacians*, Lecture Notes in Mathematics, Springer Berlin Heidelberg, 2005.
[28] J. T. Parker and P. J. Dellar, *Fourier–hermite spectral representation for the vlasov–poisson system in the weakly collisional limit*, Journal of Plasma Physics, 81 (2015).
[29] F. Poupaud and J. Soler, *Parabolic limit and stability of the vlasov–fokker–planck system*, Mathematical Models and Methods in Applied Sciences, 10 (2000), pp. 1027–1045.
[30] L. Saint-Raymond, *Hydrodynamic Limits of the Boltzmann Equation*, no. n° 1971 in Hydrodynamic Limits of the Boltzmann Equation, Springer, 2009.
[31] J. W. Schumer and J. P. Holloway, *Vlasov simulations using velocity-scaled hermite representations*, Journal of Computational Physics, 144 (1998), pp. 626–661.
[32] T. Tang, *The hermite spectral method for gaussian-type functions*, SIAM Journal on Scientific Computing, 14 (1993), pp. 594–606.
[33] C. Villani, *Hypocoercivity*, Mem. Amer. Math. Soc, 202 (2009).

Université de Toulouse & CNRS, UPS, Institut de Mathématiques de Toulouse UMR 5219, F-31062 Toulouse, France.
Email address: etienne.lehman@math.univ-toulouse.fr,claudia.negulescu@math.univ-toulouse.fr